© 2020. Published by The Company of Biologists Ltd | Development (2020) 147, dev180646. doi:10.1242/dev.180646

RESEARCH ARTICLE

JNK signaling is required for proper tangential migration and laminar allocation of cortical interneurons

Abigail K. Myers[1,2,3,‡,*], Jessica G. Cunningham[1,2,3,‡], Skye E. Smith[1,3,4], John P. Snow[3], Catherine A. Smoot[1,2,3] and Eric S. Tucker[1,3,§]

ABSTRACT

The precise migration of cortical interneurons is essential for the formation and function of cortical circuits, and disruptions to this key developmental process are implicated in the etiology of complex neurodevelopmental disorders, including schizophrenia, autism and epilepsy. We have recently identified the Jun N-terminal kinase (JNK) pathway as an important mediator of cortical interneuron migration in mice, regulating the proper timing of interneuron arrival into the cortical rudiment. In the current study, we demonstrate a vital role for JNK signaling at later stages of corticogenesis, when interneurons transition from tangential to radial modes of migration. Pharmacological inhibition of JNK signaling in *ex vivo* slice cultures caused cortical interneurons to rapidly depart from migratory streams and prematurely enter the cortical plate. Similarly, genetic loss of JNK function led to precocious stream departure *ex vivo*, and stream disruption, morphological changes and abnormal allocation of cortical interneurons *in vivo*. These data suggest that JNK signaling facilitates the tangential migration and laminar deposition of cortical interneurons, and further implicates the JNK pathway as an important regulator of cortical development.

KEY WORDS: GABAergic interneuron, Development, Forebrain, Intracellular signaling, Neuronal migration, Psychiatric disorder, Mouse

INTRODUCTION

Guided migration of cortical interneurons is mediated by the precise spatial-temporal integration of extracellular cues with intracellular signals. Failure to detect, transduce or respond to these cues can alter the abundance, distribution and connectivity of interneurons in the cerebral cortex, which may underlie severe neurological disorders such as schizophrenia, epilepsy and autism (Di Cristo, 2007; Kato and Dobyns, 2005; Marín, 2012).

Upon generation in the medial and caudal ganglionic eminences of the ventral forebrain, cortical interneurons migrate long distances to reach and infiltrate the cortical rudiment (Miyoshi et al., 2010; Nery et al., 2002; Xu et al., 2004). Within the developing cerebral cortex, interneurons predominantly travel in tangentially oriented streams located in the marginal zone (MZ), subventricular zone (SVZ) and, to a lesser extent, the subplate. As cortical development proceeds, interneurons gradually transition from tangential to radial modes of migration in order to leave their streams, layer in the cortical plate and form synaptic connections (Miyoshi and Fishell, 2011). The mechanism by which cortical interneurons mediate this tangential to radial switch appears to be multifactorial, and has been attributed to several molecular pathways, including C-X-C motif chemokine ligand 12 (Cxcl12) and its receptors Cxcr4 and Cxcr7 (Li et al., 2008; Lopez-Bendito et al., 2008; Sánchez-Alcaniz et al., 2011; Wang et al., 2011), connexin 43 (Elias et al., 2010), sonic hedgehog (Baudoin et al., 2012), and neuregulin 3 and its receptor ErbB4 (Bartolini et al., 2017). These pathways likely converge on cytoskeletal modulators, including doublecortin and $p27^{kip1}$, which have been shown to influence the dynamic behavior of migrating cortical interneurons at key choice points in their trajectories (Friocourt et al., 2007; Godin et al., 2012; Kappeler et al., 2006; Lysko et al., 2014). To date, the intracellular signaling pathways that regulate the tangential progression of cortical interneurons in migratory streams and the timing of migratory stream exit are largely unknown.

The Jun N-terminal kinases (JNKs) are a subgroup of evolutionarily conserved mitogen-activated protein kinases. Three genes, *Jnk1* (*Mapk8*), *Jnk2* (*Mapk9*) and *Jnk3* (*Mapk10*), encode JNK proteins that function to transduce stressful extracellular stimuli, as well as to enable normal physiological processes, including cell proliferation, apoptosis, differentiation and migration (Davis, 2000). JNKs are implicated in multiple aspects of brain development, including neuronal migration in the cerebral cortex (Coffey, 2014). We have previously found that JNK signaling controls the timing of interneuron entry into the cerebral cortex and the initial formation of tangential streams of migratory cells (Myers et al., 2014); however, the role that JNK plays in later stages of interneuron migration, including the tangential to radial switch, is unknown.

In the current study, we use pharmacological inhibition and genetic ablation of JNK function to investigate the role that JNK signaling plays in the tangential progression of cortical interneurons in migratory streams and the allocation of interneurons in the developing cortical wall. In live-imaging experiments from both pharmacologically treated and genetically manipulated *ex vivo* brain slices, cortical interneurons abandoned their tangential orientations, vacated streams and prematurely entered the cortical plate. Genetic loss of JNK function *in vivo* resulted in delayed entry of interneurons into the cortex at E13.5, morphological abnormalities and early stream departure of interneurons at E15.5, and incorrect positioning of calbindin-positive and calbindin-negative interneurons in the postnatal day 0 cortical wall. Our findings suggest that JNK signaling is required for the maintenance of migratory streams and that inhibition of JNK may facilitate the switch from tangential to radial

[1]Department of Neuroscience, West Virginia University School of Medicine, Morgantown, WV 26506, USA. [2]Neuroscience Graduate Program, West Virginia University School of Medicine, Morgantown, WV 26506, USA. [3]Rockefeller Neuroscience Institute, West Virginia University School of Medicine, Morgantown, WV 26506, USA. [4]Biochemistry Graduate Program, West Virginia University School of Medicine, Morgantown, WV 26506, USA.
‡These authors contributed equally to this work *Present address: Department of Pathology, Brigham and Women's Hospital, Harvard Medical School, Boston, MA 02115, USA.

§Author for correspondence (etucker@hsc.wvu.edu)

E.S.T., 0000-0003-2957-7770

Received 21 May 2019; Accepted 13 December 2019

Development (2020) 147, dev180646. doi:10.1242/dev.180646

modes of migration in order to promote the infiltration of cortical interneurons into the nascent cortical plate.

RESULTS

Loss of JNK signaling alters the radial distribution and migratory orientation of cortical interneurons

To determine whether JNK signaling is required to maintain preformed streams of migratory cortical interneurons, we cultured live-vibratome sections from E14.5 *Dlx5/6-Cre-IRES-EGFP* (*Dlx5/6-CIE*) mouse brains in either control or JNK-inhibited conditions for 12 h (Fig. 1A). Pharmacological inhibition of JNK signaling was attained using a pan-JNK inhibitor, SP600125 (Bennett et al., 2001), at concentrations previously shown to cause a delay in the entry of interneurons into the cerebral cortex (Myers et al., 2014). In control slices, interneurons travel tangentially in robust organized streams within the marginal zone (MZ) and subventricular zone (SVZ), which were preserved at both the entry zone (lateral location) and the leading edge (medial location) of cortical interneuron migration (Fig. 1B-D). In JNK-inhibited slices, interneurons disbanded from migratory streams and entered the cortical wall after treatment with 20 µM (Fig. 1E-G) and 40 µM SP600125 (Fig. 1H-J). Disruption to the MZ and SVZ streams in JNK-inhibited slices occurred throughout the entire cortex; however, significant alterations in cortical interneuron radial distribution were only present at the leading edge (Fig. 1L-M). Post-hoc analyses showed statistically significant decreases of cortical interneurons positioned in cortical bins roughly corresponding to the MZ, intermediate zone (IZ) and SVZ, as well as increases of cortical interneurons in the ventricular zone (VZ).

As radial distribution analysis indicated that interneurons from JNK-inhibited slices were displaced from their migratory streams, we asked whether their direction of migration was altered. Distributions in the orientation of leading processes were

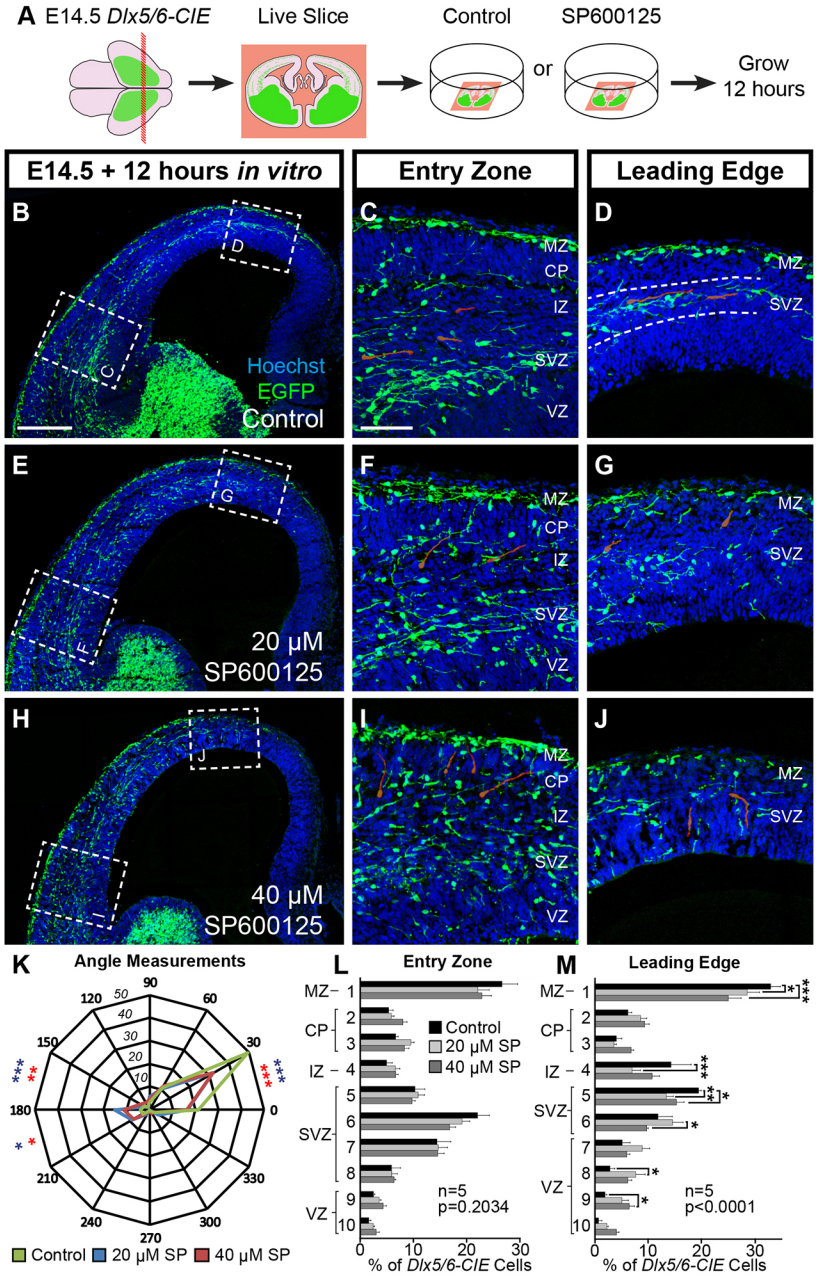

Fig. 1. JNK activity is required for cortical interneurons to remain tangentially oriented in migratory streams. (A) Schematic diagram illustrating *ex vivo* slice culture of E14.5 *Dlx5/6-CIE* brains in control or SP600125-treated conditions. (B-D) In control slices, cortical interneurons travel tangentially in migratory streams in the MZ and SVZ (dashed lines, D). (E-J) Streams are disrupted with 20 µM (E-G) and 40 µM (H-J) SP600125. Representative interneurons are highlighted in red. (K) Quantification of leading process angles. Interneurons are more tangentially oriented in control (200 cells) compared with 20 µM (178 cells; P=0.0009) and 40 µM (256 cells; P=0.0014) SP600125 conditions (χ^2 test). (L,M) Interneurons in JNK-inhibited conditions are significantly displaced at the leading edge (two-way ANOVA: $F_{(18,120)}$=3.582; P<0.0001). All analyses were performed on n=5 brains/condition from at least four experimental days. Data are mean±s.e.m. ***P<0.001, **P<0.01, *P<0.05, Fisher's LSD post-hoc test. Scale bars: 250 µm in B,E,H; 75 µm in C,D,F,G,I,J.

Development (2020) 147, dev180646. doi:10.1242/dev.180646

significantly different between control and 20 µM SP600125, and between control and 40 µM SP600125 conditions (Fig. 1K). In control conditions, 49.5% (99/200) of interneurons were tangentially oriented, whereas only 32.0% (57/178) of interneurons in the 20 µM SP600125 condition, and 32.0% (82/256) of interneurons in the 40 µM SP600125 condition, maintained a tangential orientation. Collectively, these data suggest that JNK inhibition alters the migratory trajectory of cortical interneurons and leads to their departure from migratory streams.

JNK inhibition disrupts migratory properties of cortical interneurons and causes premature departure from the SVZ stream

As fixed analyses indicated that JNK inhibition led to migratory stream departure, we performed live-imaging experiments on E14.5 *Dlx5/6-CIE* brain slices to determine whether JNK inhibition altered the dynamic behavior of migratory cortical interneurons. Unlike in control slices, where interneurons mainly traveled tangentially in migratory streams (Fig. 2A-E,K; Movie 1), cortical interneurons dramatically evacuated the SVZ stream in slices treated with 20 µM SP600125 (Fig. 2F-J,L; Movie 2). Breakdown of the SVZ stream began within a few hours of SP600125 treatment (Fig. 2G), and by 12 h, interneurons had often vacated the SVZ stream (Fig. 2J). In control slices, 74.3% (107/144) of interneurons remained in the SVZ stream, whereas in SP600125-treated slices, only 29.9% (43/144) of the tracked cortical interneurons remained. This change in migratory behavior was accompanied by significant decreases in maximum, mean, minimum and standard deviation of migratory speeds (data are mean±s.e.m.; control, max=146.5±3.28, mean=67.6±2.16, min=10.3±0.67, s.d.=37.3±0.98 µm/hour; SP600125, max=103.0±4.80, mean=41.1±3.25, min=2.88±0.53, s.d.=24.6±0.99 µm/hour; Fig. 2M), and hence an overall decrease in distance traveled (data not shown). Speed variability, which is the ratio of track standard deviation to track mean speed, was also significantly increased in JNK-inhibited conditions (control: 0.622±0.020; SP600125: 0.727±0.021; Fig. 2N). Compared with controls, migratory tracks of cortical interneurons in SP600125-treated slices were shorter in displacement over 2 h (control, 111.1±4.76 µm;

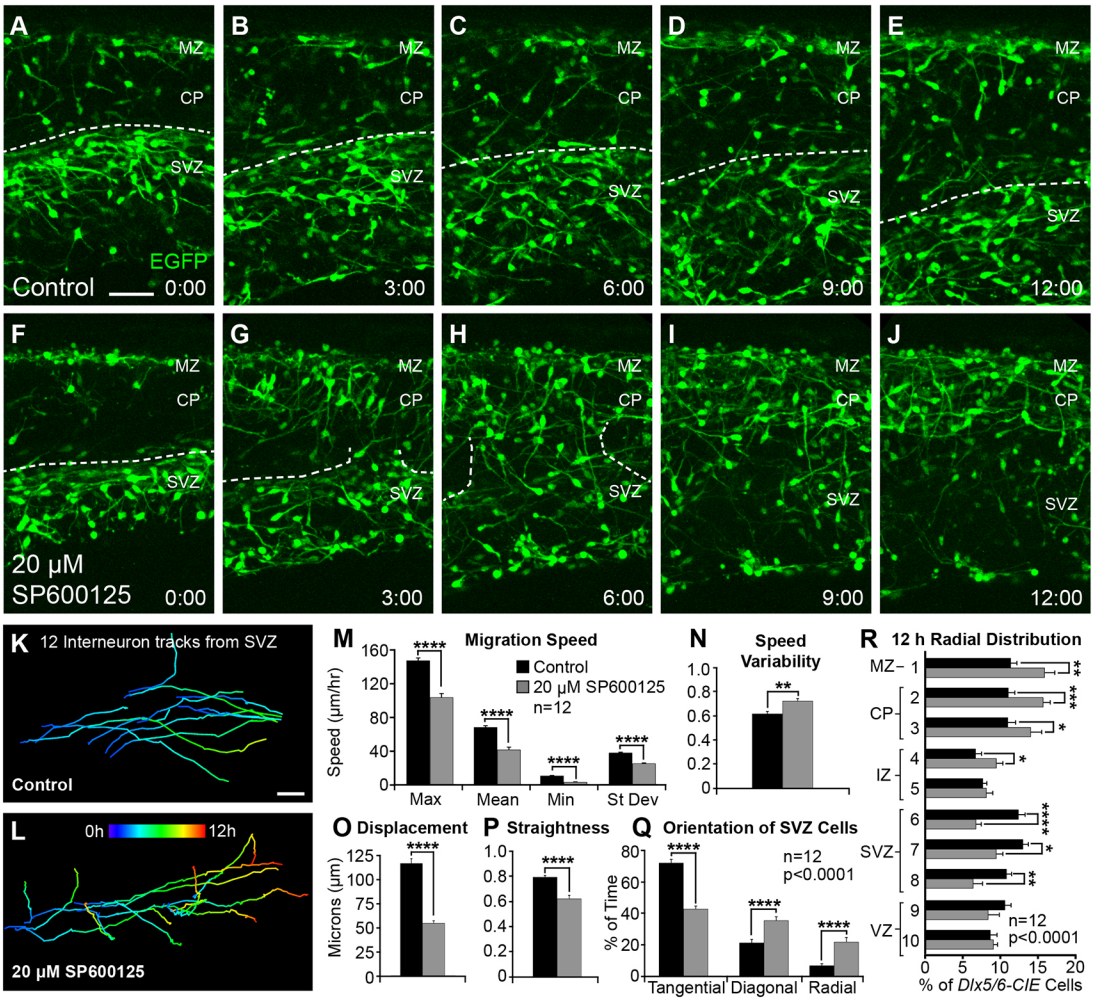

Fig. 2. Dynamic migratory properties of cortical interneurons are perturbed following pharmacological inhibition of JNK. (A-J) Movie frames from E14.5 *Dlx5/6-CIE* cortices imaged under control (A-E) or 20 µM SP600125 (F-J) conditions for 12 h *ex vivo*. Dashed lines follow the top of the SVZ stream in control conditions (A-E), and breakdown of the SVZ stream in JNK-inhibited conditions (F-J). (K,L) Tracks (pseudo-colored by time) from 12 interneurons in control (K) or 20 µM SP600125 (L) conditions. For each condition, 12 interneurons were tracked from *n*=12 movies (144 tracks/condition), generated from at least seven different embryos over 3 experimental days. (M-P) Quantification of interneuron migratory properties (Student's *t*-tests). (Q) Quantification of interneuron leading process orientations (two-way ANOVA: $F_{(2,66)}$=61.71; P<0.0001). (R) Quantification of the radial distribution of interneurons at 12 h (two-way ANOVA: $F_{(9,220)}$=7.651; P<0.0001). Data are mean±s.e.m. ****P<0.0001, ***P<0.001, **P<0.01, *P<0.05, Fisher's LSD post-hoc test. Scale bars: 50 µm.

Development (2020) 147, dev180646. doi:10.1242/dev.180646

SP600125, 51.9±2.57 µm; Fig. 2O), and had a more tortuous trajectory (track straightness: control, 0.806±0.014; SP600125, 0.631±0.027; Fig. 2P).

In addition to tracking interneuron movement, the orientation of leading processes was recorded as tangential, diagonal or radial in each movie frame (control, 3985 frames from 144 tracked cells; SP600125, 6486 frames from 144 tracked cells). The distribution of leading process orientations was significantly different between control and JNK-inhibited conditions (Fig. 2Q). Interneurons in control conditions spent 72.1±2.42% of their time in a tangential orientation, whereas JNK-inhibited interneurons spent only 42.8±1.93% of their time in a tangential orientation. Instead, JNK-inhibited interneurons spent significantly more time in both diagonal (35.5±2.45%) and radial (21.7±2.98%) orientations when compared with controls (21.2±2.27% diagonal, 6.7±1.28% radial). The non-tangential trajectories of interneuron leading processes suggest that they are leaving the SVZ stream, which was reflected in a statistically significant shift in the final overall radial distribution of interneurons in the cortical wall (Fig. 2R). Post-hoc analyses revealed a significant dispersion of interneurons from the SVZ and an accumulation of interneurons in the cortical plate (CP) and MZ after 12 h of JNK inhibition. Overall, our results indicate that JNK signaling is required to maintain the tangential orientation and migratory speed of cortical interneurons. In addition, the robust infiltration of the CP upon JNK inhibition suggests that downregulation of JNK signaling could mediate the timing of cortical interneuron departure from migratory streams and subsequent entry into the CP.

Migratory stream integrity can be partially restored after removal of JNK inhibition

In order to determine if the integrity of disrupted migratory streams could be recovered through restoration of JNK signaling, we cultured E14.5 sections for 12 h in media containing 20 µM SP600125, rinsed the slices and then cultured the slices for an additional 12 h in control media. We compared these sections to slices that were treated identically but grown in either control media or media with 20 µM SP600125 for the entire 24 h.

Interneurons in control conditions (Fig. 3A-C) predominantly maintained their location in the MZ and SVZ streams at both the entry zone and the leading edge. Compared with controls, slices treated with 20 µM SP600125 (Fig. 3D-F) contained cortical interneurons that were widely dispersed from MZ and SVZ streams, accumulating in the CP and VZ regions. When the JNK inhibitor was rinsed out after 12 h and replaced with control medium (‘washout’, Fig. 3G-I), cortical interneurons partially recovered from stream dispersion. Collectively, there were statistically significant changes in the radial distribution of interneurons between all three conditions at both the entry zone and leading edge. As expected, the SVZ showed a significant decrease in the abundance of cortical interneurons in the 20 µM SP600125 condition, indicating that JNK inhibition led to evacuation of the SVZ stream. At the entry zone and leading edge locations, there was no statistical difference in the radial distribution of interneurons between control and washout conditions in the MZ, CP and VZ regions (Fig. 3K-L), showing a recovery in the placement of interneurons that had accumulated in the CP and VZ when slices were grown in 20 µM SP600125. However, interneurons were differentially distributed within the SVZ region, showing incomplete recovery of the SVZ stream.

We also measured the angle of interneuron leading processes in all three conditions (Fig. 3J). The overall distribution of leading process angles was statistically different between the control and 20 µM SP600125 conditions, but the overall distribution was not significantly different between the control and washout conditions, indicating that interneuron orientation had partially recovered. Thus, during acute JNK inhibition of *ex vivo* slices, interneurons depart from migratory streams and have misdirected leading processes, suggesting that their ability to correctly navigate their environment is compromised. However, once JNK inhibition is removed, interneurons reorient their trajectories and partially repopulate migratory streams, indicating that their ability to respond to guidance cues located in their normal routes of migration is restored.

JNK signaling is required for interneurons to enter the cortex at the correct time *in vivo*

After finding that pharmacological loss of JNK signaling disrupted migratory streams of cortical interneurons in *ex vivo* slice cultures, we next wanted to determine whether the complete genetic loss of JNK function from interneurons disrupts interneuron migration *in vivo*. *Jnk1;Jnk2* double mutants are early embryonic lethal (Kuan et al., 1999), and combinatorial loss of *Jnk1* and *Jnk2* has a greater effect on interneuron migration than loss of *Jnk1* alone (Myers et al., 2014). We therefore developed two conditional knockout models in which *Jnk1* was removed from interneurons using a *Dlx5/6-CIE* driver in either a constitutive *Jnk2*-null background (conditional double knockout, *cDKO*: *Dlx5/6-CIE; Jnk1*$^{fl/fl}$*; Jnk2*$^{-/-}$) or in a constitutive *Jnk2;Jnk3* double-null background (conditional triple knockout, *cTKO*: *Dlx5/6-CIE; Jnk1*$^{fl/fl}$*; Jnk2*$^{-/-}$*; Jnk3*$^{-/-}$) in order to completely eliminate JNK signaling in interneurons. In previous work (Myers et al., 2014), we showed that at different rostrocaudal levels, interneurons in *cDKO* cortices had a delayed entrance into the cortex when compared with embryos heterozygous for the conditional deletion of *Jnk1* in a *Jnk2*-null background (*cHKO*: *Dlx5/6-CIE; Jnk1*$^{fl/+}$*; Jnk2*$^{-/-}$) at E13.5. In order to determine whether the entry of interneurons into the cortex was similarly disrupted in *cTKO* embryos at E13.5, we compared *cTKO*, *cHKO* and *cDKO* genotypes (Fig. 4A-C), and found a statistically significant interaction between genotype and bin location (Fig. 4E). Moreover, we observed an allelic dose effect in the requirement for JNK in interneuron entry into the cortex (Fig. 4A-C,E). Post-hoc analyses revealed that there were significant increases in the proportion of interneurons located at the entry zone, as well as significant decreases in the proportion of interneurons reaching more medial cortical positions when Jnk genes were progressively eliminated. These data indicate that genetic removal of *Jnk1*, *Jnk2* and *Jnk3* leads to an even more pronounced delay in interneuron entry into the E13.5 cortex than removal of *Jnk1* and *Jnk2*.

Surprisingly, we found that, by E15.5, interneurons had advanced to the same location in the medial cortex of all three genotypes, indicating that cortical interneurons recover from their initial delay at E13.5 (Fig. 4F-H, arrows). After observing a similar medial advancement in the *cHKO* and *cDKO* cortices at E15.5, we quantitatively assessed the radial distribution of cortical interneurons at lateral, mid and medial cortical locations, and found no statistical differences between these two genotypes (Fig. S1). The apparent recovery of interneuron advancement and stream integrity in the *cDKO* cortex compared with the *cHKO* cortex allowed us to compare interneurons between *cDKO* and *cTKO* cortices to determine whether the additional removal of *Jnk3* in *cTKO* embryos further impairs their development.

Development (2020) 147, dev180646. doi:10.1242/dev.180646

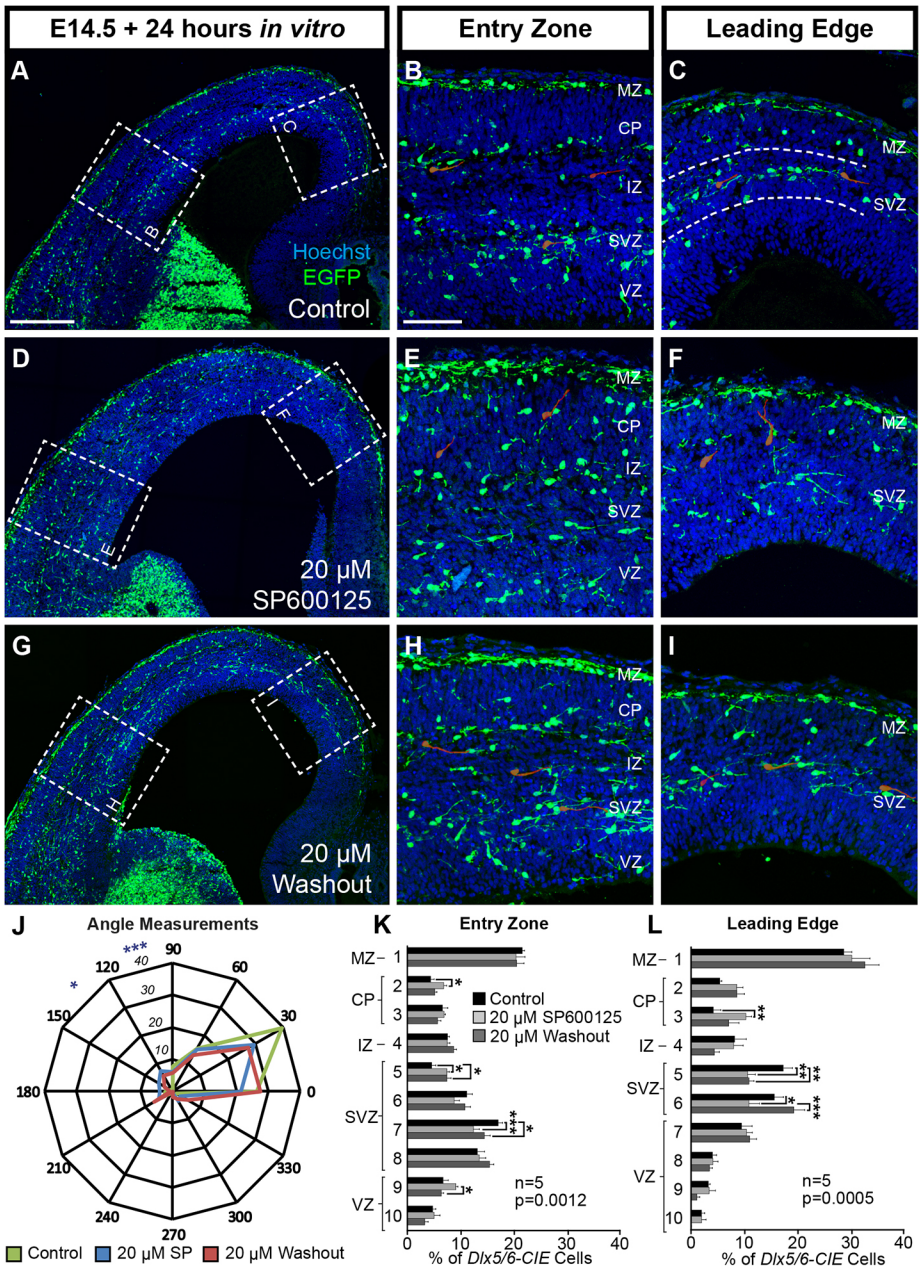

Fig. 3. Migratory stream integrity partially recovers after removal of JNK inhibitor. (A-C) Migratory streams remain intact (dashed lines, C) when slices are grown in control conditions for 24 h. (D-F) MZ and SVZ streams are disrupted when slices are grown in 20 μM SP600125. (G-I) Partial recovery of the SVZ stream is observed when slices are grown in 20 μM SP600125 for 12 h, rinsed and then grown in control media for an additional 12 h ('washout'). Representative interneurons are highlighted in red. (J) Quantification of leading process angles. Differences are found between control (129 cells) and 20 μM SP600125 (178 cells; P=0.031), but not between the control and washout (106 cells; P=0.065) conditions (χ^2 test). (K,L) Stream dispersion partially recovers in the washout condition (two-way ANOVA; entry zone $F_{(18,120)}$=2.579, P=0.0012; leading edge $F_{(18,120)}$=2.785; P=0.0005). All analyses were performed on n=5 brains/condition from 5 experimental days. Data are mean±s.e.m.. ***P<0.001, **P<0.01, *P<0.05, Fisher's LSD post-hoc test. Scale bars: 250 μm in A,D,G; 75 μm in B,C,E,F,H,I.

Genetic loss of JNK signaling alters interneuron distribution and morphology

Despite an apparent recovery in the medial advancement of interneurons in the E15.5 cortex, we found that the integrity of migratory steams was disrupted in *cTKO* brains (Fig. 5). Gaps were present in the MZ and SVZ streams throughout the lateral to medial extent of the cortex (Fig. 5E-F), suggesting that interneurons were missing or displaced from their normal positions. Some *cTKO* brains had even more severe disruptions, including prominent clusters of interneurons extending from the MZ, or aggregations of interneurons in the subplate region (Fig. S2G,I). *cTKO* brains that contained large clusters of interneurons also displayed obvious disruptions to the developing cortical wall (Fig. S2H). We excluded *cTKO* brains from our analyses that contained prominent dipped regions of the cortical plate, as this dysmorphic feature impeded our ability to accurately measure the radial distribution of interneurons. When the remaining *cTKO* brains were compared with *cDKO* brains, we found the overall radial distribution of cortical interneurons was significantly altered in the E15.5 *cTKO* cortical wall (Fig. 5I). The lower SVZ contained fewer interneurons in the *cTKO* cortex, while the upper SVZ contained more, suggesting that interneurons were prematurely departing from the SVZ stream.

Morphological alterations in the leading processes and/or cell bodies of cortical interneurons could indicate a disruption in their migratory properties (Baudoin et al., 2008; Bellion et al., 2005; Martini and Valdeolmillos, 2010). To determine whether the genetic loss of JNK signaling impacted interneuron morphology, we first measured the length of leading processes of individual interneurons located between the SVZ and MZ streams at E15.5. The average leading process length from *cDKO* interneurons was statistically longer than in *cTKO* interneurons (*cDKO*: 17.8±1.10 μm; *cTKO*: 13.1±0.82 μm; Fig. 5L). Additionally, by measuring the circularity of interneuron soma, we found *cTKO* interneurons to be significantly more spherical than interneurons in

Development (2020) 147, dev180646. doi:10.1242/dev.180646

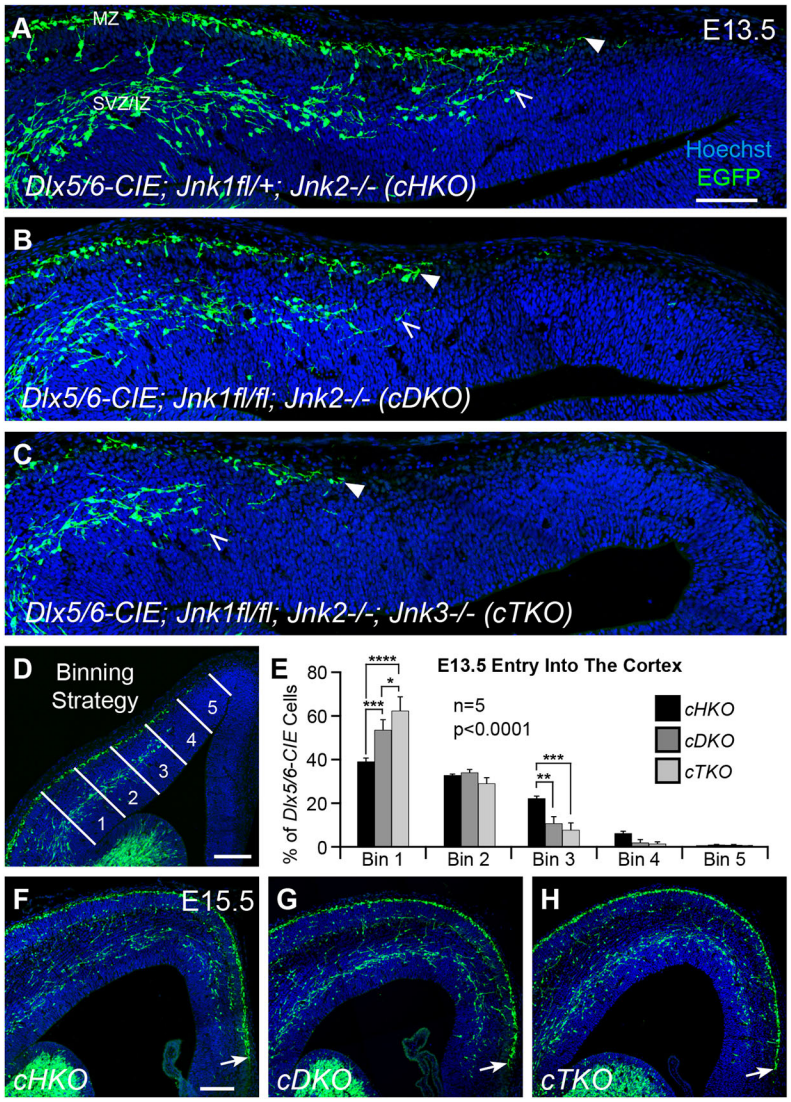

Fig. 4. Arrival of interneurons into the cortex is transiently delayed by genetic removal of JNK function *in vivo*. (A-C) At E13.5, interneuron entry (MZ stream, closed arrowheads; SVZ stream, open arrowheads) is progressively delayed into the cortex with the stepwise removal of JNK function *in vivo*. (D,E) Quantification of interneuron distribution in five equidistant bins (lateral to medial) was performed on n=5 brains/genotype (two-way ANOVA: $F_{(8,60)}$=7.52; P<0.0001). (F-H) Interneurons in all three genotypes have advanced to a similar location in the medial cortical wall by E15.5 (arrows). Data are mean±s.e.m. ****P<0.0001, ***P<0.001, **P<0.01, *P<0.05, Fisher's LSD post-hoc test. Scale bars: 100 µm in A-C; 150 µm in D,F-H.

cDKO cortices (*cTKO*, 0.741±0.0038; *cDKO*, 0.695±0.010; Fig. 5M). No statistical differences were found in either the area or perimeter of the interneuron cell bodies (data not shown), suggesting that their overall size remained unchanged. Interestingly, in brains with cortical malformations, we found many interneurons with short, blebby leading processes, as well as very spherical cell bodies (Fig. S2I, arrowheads), suggesting interneuron morphology was more affected in these brains.

Taken together, our data indicate that complete genetic removal of JNK signaling from cortical interneurons in a *Jnk2;Jnk3* deficient environment leads to irregularities in migratory streams that are evident by E15.5 *in vivo*, as well as morphological alterations to interneurons that are consistent with disrupted migratory properties.

Genetic removal of JNK alters the dynamic migratory properties of cortical interneurons in *ex vivo* slices

We next assessed whether the dynamic properties of cortical interneurons changed with genetic ablation of JNK signaling. When organotypic brain slices from E14.5 embryos were imaged for 18 h *ex vivo*, many interneurons in *cDKO* slices maintained tangential progression in migratory streams throughout the entire imaging period (Fig. 6A-E; Movie 3). In contrast, fewer interneurons maintained tangential progression over the 18 h imaging period in *cTKO* slices (Fig. 6F-J; Movie 4), and many more *cTKO* interneurons departed from migratory streams in the last 6 h of imaging (Fig. 6H-J). Only 46.0% (138/300) of all tracked cortical interneurons remained in the SVZ stream in *cTKO* slices, whereas 59.7% (179/300) remained in *cDKO* slices. In order to determine whether the requirement for JNK differed during the 18 h of imaging, we analyzed interneuron migration in three 6 h intervals (0-6 h, 6-12 h and 12-18 h, pseudocolored to represent time; Fig. 6K-M). We found that changes in the dynamic behavior of *cDKO* and *cTKO* interneurons were most pronounced during the 12-18 h time frame, when interneurons normally begin to exit streams.

Unlike with pharmacological JNK inhibition, alterations in the track behavior of *cTKO* interneurons were not accompanied by statistically significant reductions in migratory speed (*cDKO*, max=123.3±5.12, mean=57.9±2.76, min=8.98±0.84, s.d.=32.0±1.54 µm/hour; *cTKO*, max=121.7±3.7, mean=51.1±2.02, min=7.08±0.96, s.d.=32.2±1.01 µm/hour; Fig. 6N), or a corresponding reduction in overall track length (data not shown). When examining track speed variability, however, there was a statistical difference between *cDKO* and *cTKO* interneurons (*cDKO*, 0.642±0.024; *cTKO*, 0.752±0.022; Fig. 6O), suggesting that *cTKO* interneurons are not traveling at consistent speeds along their migratory tracks. Similar to

Development (2020) 147, dev180646. doi:10.1242/dev.180646

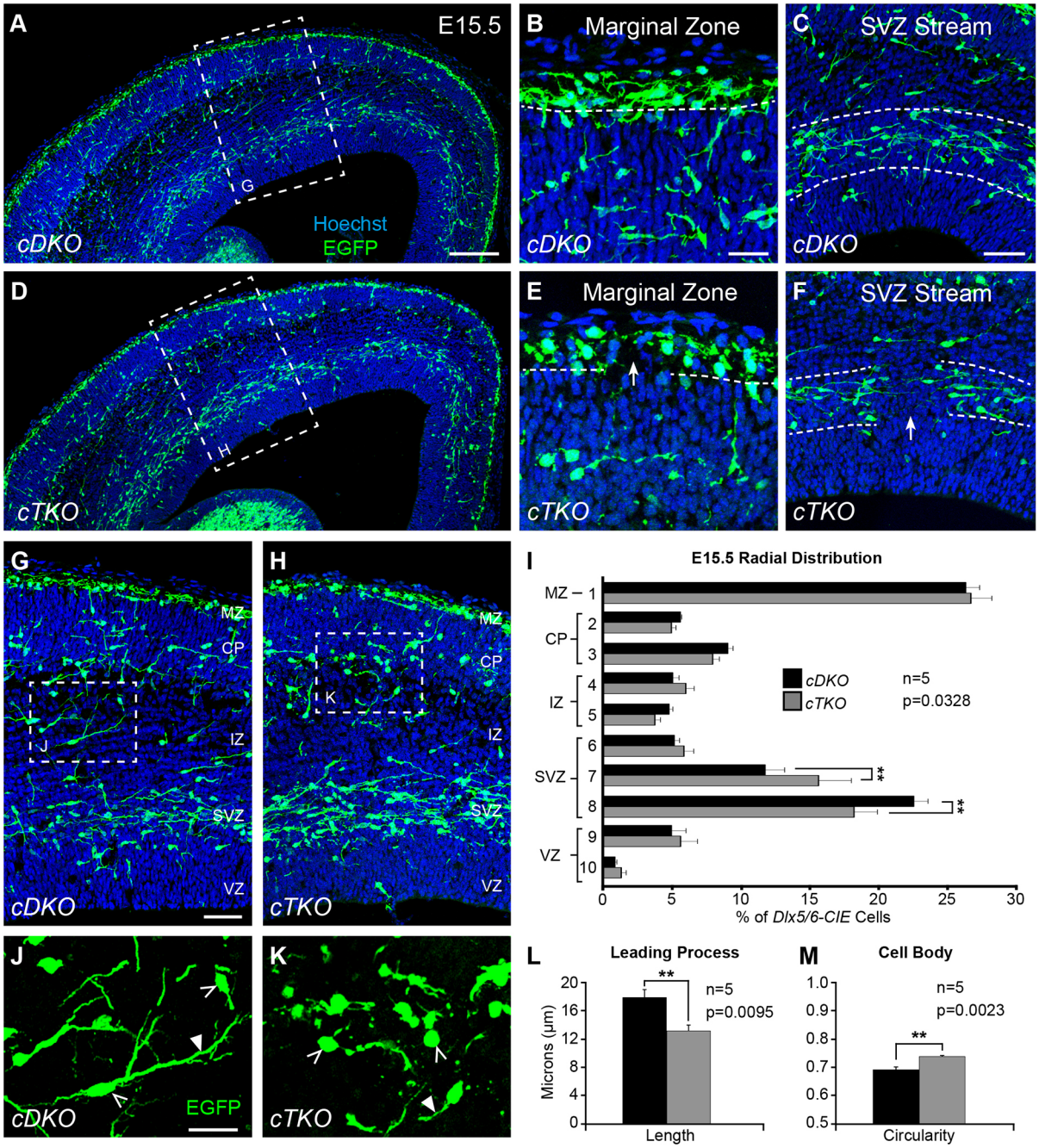

Fig. 5. Genetic loss of JNK signaling results in interneuron stream displacement and morphological changes at E15.5. (A-C) In conditional double knockout (*cDKO*) cortices, interneurons travel in organized streams in the MZ (B) and SVZ (C). (D-F) In conditional triple-knockout (*cTKO*) cortices, frequent gaps are found in the MZ (E) and SVZ (F) streams (arrows). (G-I) Quantification of interneuron distribution in the cortical wall from n=5 brains/genotype (two-way ANOVA: $F_{(9,80)}$=2.17; P=0.0328). (J-M) Quantification of interneuron morphology from n=5 brains/genotype (Student's t-tests). *cTKO* interneurons (430 cells) have shorter leading processes (closed arrowheads) than *cDKO* interneurons (510 cells), and *cTKO* interneurons (656 cells) have more circular cell bodies (open arrowheads) than *cDKO* interneurons (787 cells). Data are mean±s.e.m. **P<0.01, Fisher's LSD post-hoc test. Scale bars: 150 µm in A,D; 25 µm in B,E,J,K; 50 µm in C,F,G,H.

pharmacological inhibition of JNK, *cTKO* interneurons had an overall shorter displacement (*cDKO*, 92.3±5.09 µm; *cTKO*, 75.7±3.39 µm; Fig. 6P) and less straight trajectories (*cDKO*, 0.773±0.011; *cTKO*, 0.718±0.020; Fig. 6Q). Additionally, when we assessed the amount of time that the leading processes of migrating interneurons were oriented tangentially, diagonally or radially in each movie frame (*cDKO*, 2266 frames from 100 tracks; *cTKO*, 2441 frames from 100 tracks), we found statistically significant differences between the two genotypes (Fig. 6R). *cTKO* interneurons spent significantly less time orientated tangentially (26.2±1.94%) compared with *cDKO* interneurons (40.9±3.73%), and significantly more time orientated diagonally (*cTKO*, 51.9±2.15%; *cDKO*, 43.4±0.84%). This finding supports our observation that more interneurons are leaving streams and are angled upwards towards the CP region of *cTKO* slices. Together, these data indicate that genetic loss of JNK signaling alters the migratory behavior of cortical interneurons in *ex vivo* slices of

Development (2020) 147, dev180646. doi:10.1242/dev.180646

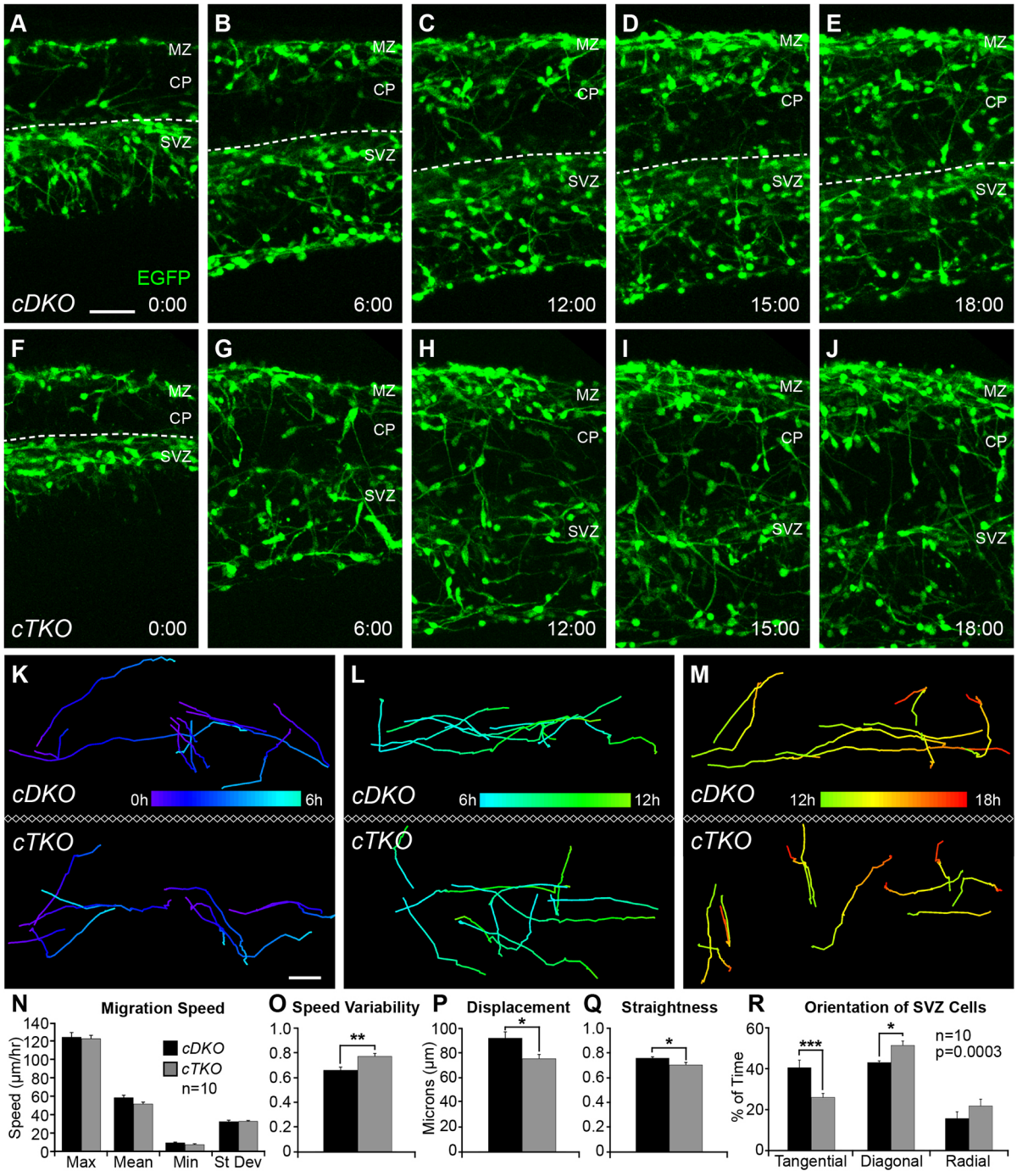

Fig. 6. Dynamic properties of migrating interneurons are disrupted in *ex vivo* slices from *cTKO* brains. (A-E) Movie frames from E14.5 *cDKO* cortices imaged for 18 h *ex vivo*. Dashed line represents the top of the SVZ stream. (F-J) Movie frames from *cTKO* cortices show premature disbanding of interneurons from migratory streams. (K-M) Representative tracks (pseudo-colored by time) from interneurons recorded at 0-6 h (K), 6-12 h (L) and 12-18 h (M) in *cDKO* and *cTKO* slices. Ten interneurons were tracked during each time interval for a total of 30 tracks/movie, 300 tracks/genotype. Movies (n=10) collected from five different embryos/genotype on four experimental days were used for analyses. (N-Q) Quantification of interneuron dynamics during the 12-18 h time interval (Student's t-tests). (R) Quantification of interneuron leading process orientations (two-way ANOVA: $F_{(2,54)}$=9.63; P=0.0003). Data are mean±s.e.m. ***P<0.001, **P<0.01, *P<0.05, Fisher's LSD post-hoc test. Scale bars: 50 μm.

cTKO brains, resulting in tracks with more variable migratory speeds, and more tortuous, misrouted trajectories that increase in severity as development proceeds.

As our dynamic imaging data revealed that the migratory trajectories of *cTKO* interneurons worsened over time, we sought to determine whether this change in migratory behavior led to a gradual redistribution of interneurons in *ex vivo* slices (Fig. 7). Initially, no differences in interneuron distribution were observed between E14.5 *cDKO* and *cTKO* cortices at the 0 h time point (Fig. 7A-C). However, robust redistribution of *cTKO* interneurons was evident by the end of the 18 h imaging period (Fig. 7D-F). Post-hoc analyses revealed that there were significant decreases in the abundance of interneurons from the SVZ region of *cTKO* cortices, and concomitant increases in the abundance of interneurons in the

Development (2020) 147, dev180646. doi:10.1242/dev.180646

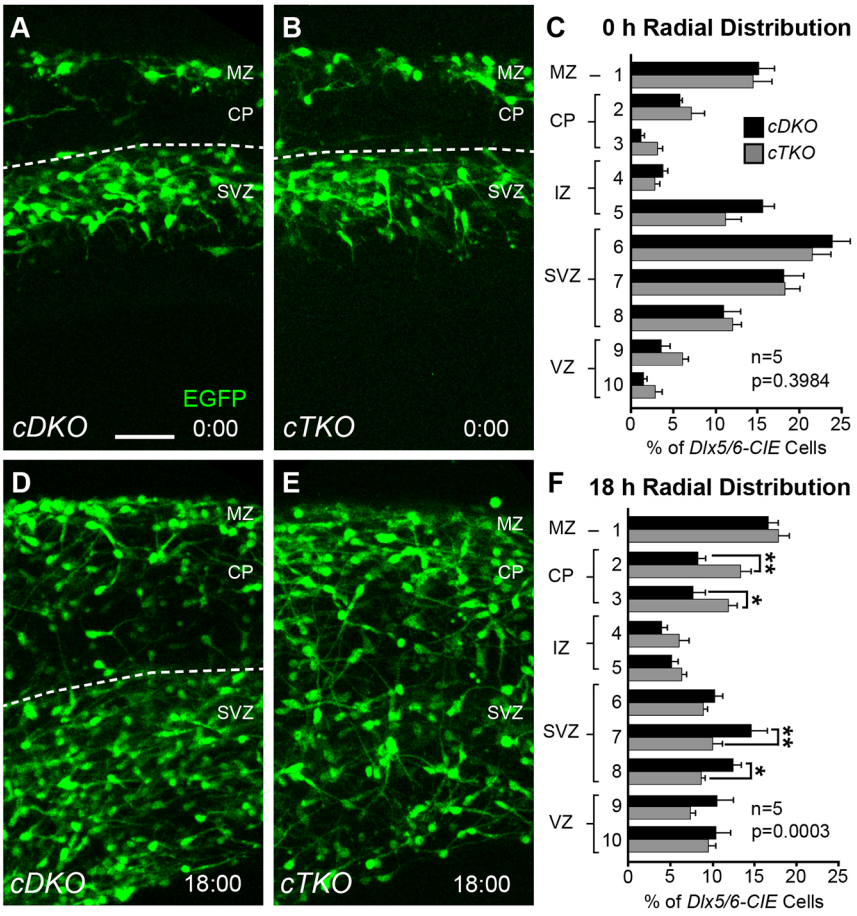

Fig. 7. Cortical interneurons gradually disperse from migratory streams in *cTKO* cortices. (A,B,D,E) Movie frames from 0 and 18 h timepoints captured from E14.5 *cDKO* and *cTKO ex vivo* cortices. Dashed line represents the top of the SVZ stream. (C,F) Quantification (n=5 brains/genotype) of the radial distribution of interneurons reveals no difference at 0 h, but significant redistribution by 18 h (two-way ANOVA: $F_{(9,80)}$=4.06, P=0.0003). Data are mean±s.e.m. **P<0.01, *P<0.05, Fisher's LSD post-hoc test. Scale bar: 50 µm.

CP region. These data suggest genetic elimination of JNK signaling leads to a premature accumulation of cortical interneurons in the CP.

JNK-depleted interneurons are incorrectly distributed in the early postnatal cortex

We next wanted to determine whether the early disbanding of interneurons from migratory streams led to long-lasting alterations in their laminar distribution. Although attempts to rear *cTKO* pups into adulthood proved unsuccessful, we were able to recover live animals at postnatal (P) day 0 in expected Mendelian ratios and analyze their cortices (Fig. 8). Similar to E15.5, some *cTKO* brains contained cortical malformations at P0, which were variable in size and location (data not shown). We used the mid-cortical position at the level of the anterior commissure to examine the distribution of interneurons, as gross malformations in the cortical plate were not detectable at this location. When we compared the radial distribution of interneurons between *cDKO* and *cTKO* cortices at P0 (Fig. 8A,B), we found statistically significant alterations in their placement (Fig. 8E). Post-hoc analyses revealed that interneurons in *cTKO* cortices were most prominently reduced in the VZ/SVZ, and elevated in the lower CP and MZ regions. In order to determine whether alterations in interneuron placement were consistent across interneuron subtypes, we examined the positioning of calbindin-labeled cortical interneurons in the P0 cortical wall (Fig. 8C,D). Statistically significant alterations in the radial distribution of calbindin-GFP double-labeled cells were observed between *cDKO* and *cTKO* cortices (Fig. 8F), with post-hoc analyses identifying significant reductions in the VZ and elevations in the lower CP regions. Interestingly, calbindin-GFP double-labeled cells did not accumulate in the MZ region, where GFP-positive cells also accumulated in *cTKO* brains (Fig. 8E, bin 1). Indeed, we found a striking increase of GFP-positive calbindin-negative interneurons (open arrowheads in Fig. 8C-D) in the MZ region of *cTKO* cortices (Fig. 8G, bin 1), suggesting that changes to the distribution of the calbindin-labeled cortical interneurons do not fully account for interneuron allocation defects in *cTKO* brains. Together, our data suggest that migratory anomalies occurring during embryonic development lead to lamination defects that persist until P0 in *cTKO* mice, and that the laminar re-distribution of cortical interneurons in *cTKO* cortices does not uniformly influence all interneuron subtypes.

Assessing autonomy for JNK function in interneuron migration and allocation

Although our data support a role for JNK in the migration and laminar positioning of cortical interneurons, it is not clear whether interneurons have a cell-intrinsic requirement for JNK signaling, or whether genetic and pharmacological inhibition of JNK disrupts interneuron migration through non-autonomous mechanisms. In the *cTKO* model, JNK is completely eliminated from cortical interneurons; however, *Jnk2* and *Jnk3* are constitutively deleted from the entire animal, which means JNK-depleted interneurons must navigate a partially JNK-deficient environment into and within the cortical rudiment. In order to determine whether the *Jnk2* and *Jnk3* double-knockout environment could itself lead to interneuron migration anomalies, we compared the allocation of *Dlx5/6-CIE* cortical interneurons between wild-type and *Jnk2;Jnk3* double-knockout mice at P0. We did not find statistically significant

Development (2020) 147, dev180646. doi:10.1242/dev.180646

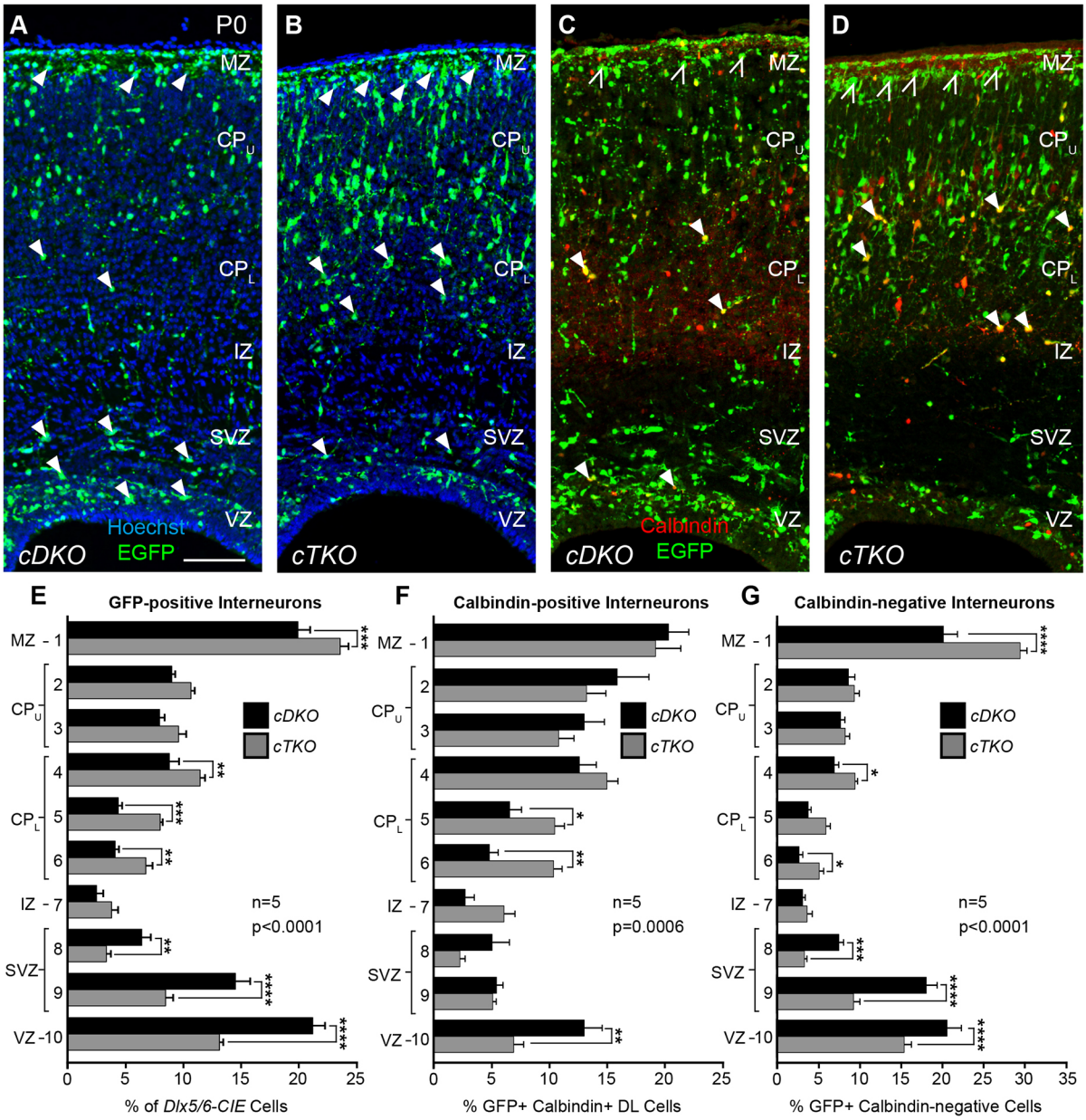

Fig. 8. Cortical interneurons are mispositioned in the early postnatal cortex of *cTKO* mice. (A,B) GFP-positive (*Dlx5/6-CIE*) interneurons in the *cDKO* (A) and *cTKO* (B) cortical wall. (C,D) GFP-calbindin double-labeled (DL) interneurons in the *cDKO* (C) and *cTKO* (D) cortical wall. (E-G) Quantification of the radial distribution of GFP-positive (E; two-way ANOVA: $F_{(9,80)}$=20.33, P<0.0001), DL (F; two-way ANOVA: $F_{(9,80)}$=3.700, P=0.0006) and GFP-positive calbindin-negative (G; two-way ANOVA: $F_{(9,80)}$=18.77, P<0.0001) interneurons. GFP-positive interneurons are reduced in the VZ/SVZ and are elevated in the lower cortical plate (CP_L) and marginal zone (MZ) of the *cTKO* cortical wall (arrowheads in A,B). DL interneurons are reduced in the VZ and elevated in the CP_L of the *cTKO* cortical wall (closed arrowheads, C,D), but unchanged in the MZ. GFP-positive calbindin-negative interneurons are increased in the MZ (open arrowheads in C,D). Quantification from n=5 brains/genotype. Data are mean±s.e.m. ****P<0.0001, ***P<0.001, **P<0.01, *P<0.05, Fisher's LSD post-hoc test. Scale bar: 100 µm.

alterations in the distribution of *Dlx5/6-CIE* interneurons between these genotypes (Fig. 9A,B,D), suggesting that loss of *Jnk2* and *Jnk3* is insufficient to alter interneuron allocation. Moreover, when we compared the distribution of interneurons in mice that conditionally eliminated only one copy of *Jnk1* from a *Jnk2;Jnk3* double-knockout background (Fig. 9C), we found statistically similar distributions of interneurons to those in wild-type and *Jnk2;Jnk3* mutant cortices (Fig. 9D). However, interneuron distribution in *cTKO* brains (Fig. 8B) was statistically different from wild type (Fig. 9A; $F_{(9,60)}$=12.73; P<0.0001), *Jnk2;Jnk3* double knockout (Fig. 9B; $F_{(9,60)}$=18.12; P<0.0001) and even *Jnk2;Jnk3* double knockouts missing one copy of *Jnk1* from *Dlx5/6-CIE* cells (Fig. 9C; $F_{(9,60)}$=13.39; P<0.0001 by two-way ANOVA). These findings suggest defects in interneuron positioning are present only when JNK is completely eliminated from interneurons in *cTKO* brains.

Finally, as pharmacological inhibition of JNK in *ex vivo* slice cultures disrupts JNK signaling in all cell types within the slice, we asked whether JNK inhibition could impair the migration of interneurons when they are grown alone. We grew explants of medial ganglionic eminence (MGE) tissue in 3D Matrigel cultures for 1 day, added control medium or medium containing 20 µM

Development (2020) 147, dev180646. doi:10.1242/dev.180646

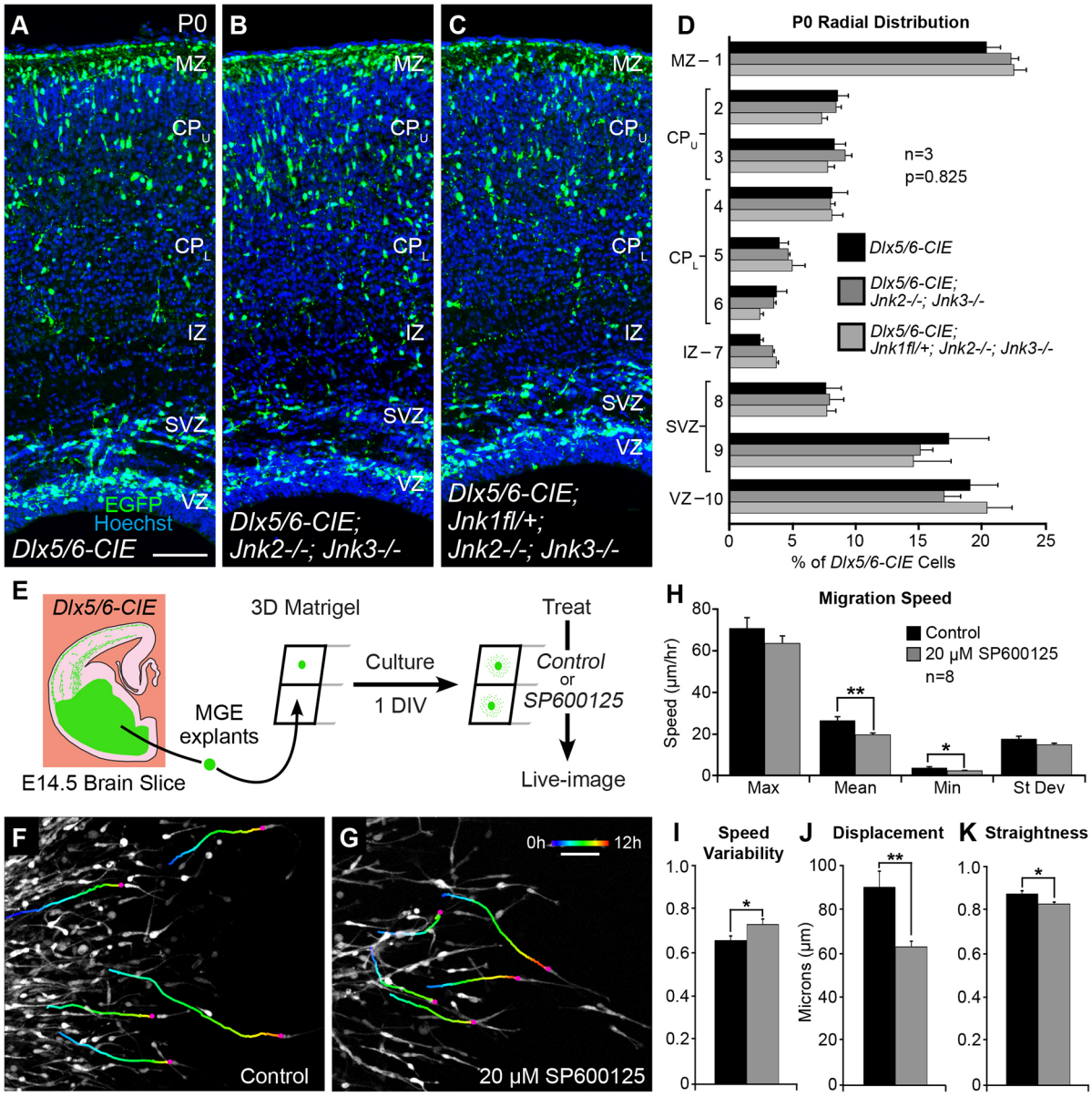

Fig. 9. Cortical interneurons appear to have a cell-intrinsic requirement for JNK signaling. (A-D) *Dlx5/6-CIE*, *Dlx5/6-CIE; Jnk2*$^{-/-}$*;Jnk3*$^{-/-}$ and *Dlx5/6-CIE; Jnk1*$^{fl/+}$*;Jnk2*$^{-/-}$*;Jnk3*$^{-/-}$ cortices have statistically similar distributions of cortical interneurons, *n*=3 brains/genotype. (E) E14.5 *Dlx5/6-CIE* medial ganglionic eminence (MGE) explants are grown in a 3D Matrigel assay for 1 day *in vitro* (DIV), treated with control or 20 µM SP600125 media, and then imaged live for 12 h. (F,G) Tracks (pseudo-colored by time) from five representative interneurons in control and 20 µM SP600125 conditions. For each condition, 10 interneurons were tracked from *n*=8 movies (80 tracks/condition) collected from three experiments. (H-K) Quantification of dynamic interneuron properties. Data are mean ±s.e.m. ***P*<0.01, **P*<0.05, Student's *t*-tests. Scale bars: 100 µm in A-C; 50 µm in F,G.

SP600125, then imaged interneurons live for 12 h (Fig. 9E-G; Movies 5 and 6). By tracking cells in both conditions, we found JNK inhibition in MGE explant cultures to impair the migratory properties of cortical interneurons. When compared with controls, JNK-inhibited interneurons displayed statistically significant alterations in mean and minimum migratory speeds (control, max=70.4±5.11, mean=25.8±1.92, min=3.40±0.59, s.d.=17.0±1.39 µm/hour; SP600125, max=63.4±3.53, mean=19.2±0.84, min=2.03±0.24, s.d.=14.4±0.77 µm/hour; Fig. 9H), speed variability (control, 0.680±0.021; SP600125, 0.755±0.026; Fig. 9I), displacement (control, 90.9±7.37 µm; SP600125, 63.6±2.59 µm; Fig. 9J) and track straightness (control, 0.872±0.015; SP600125, 0.826±0.009; Fig. 9K). These findings suggest that the migratory behavior of cortical interneurons at least partially relies on a cell-intrinsic requirement for JNK signaling.

DISCUSSION

We found that tangential progression of cortical interneurons in migratory streams depends on the JNK signaling pathway. Pharmacological inhibition of JNK signaling in E14.5 slices resulted in dispersion of cortical interneurons from pre-formed migratory streams, which was partially recoverable upon removal of the inhibitor. Live imaging revealed that acute JNK inhibition led to rapid stream departure, as JNK-inhibited cortical interneurons switched from tangential to radial modes of migration, exited the SVZ stream and infiltrated the cortical plate. To genetically

Development (2020) 147, dev180646. doi:10.1242/dev.180646

eliminate JNK from interneurons, we developed conditional triple knockout (*cTKO*) mice, which removed *Jnk1* from interneurons of *Jnk2;Jnk3* double knockouts. Live imaging of *cTKO* slice cultures at E14.5 recapitulated our *ex vivo* pharmacological data by showing an increase in non-tangential migratory trajectories, evacuation of the SVZ stream and premature accumulation of interneurons in the cortical plate. In *cTKO* cortices *in vivo*, interneurons were delayed in their arrival to the cortex at E13.5 and were displaced from migratory streams at E15.5. At P0, we found that interneurons in *cTKO* cortices had vacated the VZ/SVZ and overpopulated deeper layers of the CP and MZ, and that distinct subtypes of cortical interneurons accumulated differently in the JNK-deficient cortical wall. Finally, we provided genetic and pharmacological evidence that disrupted migration and allocation of cortical interneurons at least partially relies on cell-intrinsic requirements for JNK signaling. Together, our results suggest that JNK signaling maintains the integrity of cortical interneuron migratory streams and enables the correct positioning of interneurons in the cortical wall.

Molecular mechanisms underlying cortical plate invasion by interneurons

The JNK signaling pathway might facilitate interneuron departure from migratory streams by intersecting with other known mediators of cortical plate invasion. The chemokine Cxcl12 is expressed along the migratory routes of cortical interneurons and helps to establish and maintain migratory streams in the developing cortex (Stumm et al., 2003; Tham et al., 2001; Tiveron et al., 2006). Chemoattraction to Cxcl12 is mediated by the activity of two chemokine receptors, Cxcr4 and Cxcr7, which are expressed by migrating cortical interneurons (Lopez-Bendito et al., 2008; Sánchez-Alcaniz et al., 2011; Wang et al., 2011). Pharmacological loss of Cxcr4 function in other studies (Lysko et al., 2011; Wang et al., 2011), and the JNK pathway here, results in migratory stream departure and the precocious entry of interneurons into the cortical plate. *Cxcr4*-, *Cxcr7*- and *Cxcl12*-null mice have disrupted migratory streams and persistent alterations to cortical interneuron distribution (Abe et al., 2014; Lopez-Bendito et al., 2008; Sánchez-Alcaniz et al., 2011; Wang et al., 2011), which closely parallel our findings in *cTKO* cortices. Additionally, in both *Cxcr7*-null (Wang et al., 2011) and *cTKO* mice, interneurons have morphological alterations, including shorter, less tangentially oriented leading processes. These similarities, along with other studies indicating that Cxcr4 signaling can activate JNK to induce migration in non-neuronal cells (Décaillot et al., 2011; Liao et al., 2015), suggest that JNK may act downstream of chemokine signaling to modulate the formation and maintenance of migratory streams. Thus, as interneuron responsiveness to Cxcl12 diminishes, a key feature thought to mediate migratory stream departure (Li et al., 2008), JNK levels may decline to enable the tangential to radial switch.

Mechanisms outside of chemokine signaling also appear to regulate cortical plate invasion. Connexin 43 (Cx43), a gap junction protein, participates in the tangential to radial transition by promoting adhesion between cortical interneurons and radial glial cells (Elias et al., 2010). Studies in cardiomyocytes suggest that JNK activation downregulates the expression of Cx43 (Petrich et al., 2002). In interneurons, downregulation of Cx43 decreases interneuron entry into the cortical plate (Elias et al., 2010). Therefore, developmental reduction of JNK activity could promote migratory stream exit by increasing the expression of Cx43 in migrating cortical interneurons. Additionally, other extrinsic factors may reinforce cortical plate invasion. For example, sonic hedgehog (Shh) is expressed at low levels in the developing cortex, and treatment of cortical slices with Shh results in stream dispersion and cortical plate accumulation (Baudoin et al., 2012), reminiscent of the stream departure seen after JNK inhibition. Similarly, neuregulin 3 (Nrg3) is expressed by excitatory neurons in the developing cortex (Bartolini et al., 2017) and is a ligand for ErbB4, a receptor tyrosine kinase expressed by migrating cortical interneurons (Flames et al., 2004; Yau et al., 2003). Overexpression of Nrg3 promotes migratory stream departure, and conditional deletion of *Nrg3* or *Erbb4* alters the laminar allocation of interneurons in the postnatal cortex (Bartolini et al., 2017). Thus, it is possible that activation of these pathways reduces JNK activity in cortical interneurons or that reduced JNK activity facilitates Shh and ErbB4-mediated migratory stream departure, but additional experiments are needed to test these models.

Diverse requirements for JNK during cortical interneuron migration

Complex migratory decisions, such as choosing when and where to depart from migratory streams, likely involve the coordination of extrinsic and intrinsic molecular signals. As JNKs are expressed in both interneurons and other cells of the cortical environment (Myers et al., 2014), JNK signaling may influence interneurons through both autonomous and non-autonomous mechanisms. One means by which JNK could exert a cell autonomous influence on cortical interneuron migration is through modulation of the cytoskeleton. For example, doublecortin, a microtubule-binding protein known to regulate leading process branching and guided migration of cortical interneurons (Friocourt et al., 2007; Kappeler et al., 2006), is a downstream target of JNK signaling (Gdalyahu et al., 2004; Jin et al., 2010). Additionally, $p27^{kip1}$ is a microtubule-associated protein that coordinates microtubule polymerization and actomyosin contraction to attune leading process branching and nucleokinesis (Godin et al., 2012). Conditional deletion of $p27^{kip1}$ from post-mitotic cortical interneurons delays cortical entry at E12.5 (Godin et al., 2012), similar to our observations following loss of JNK. During cancer cell migration, JNK signaling regulates cell-cell adhesions via $p27^{kip1}$ phosphorylation (Kim et al., 2012), suggesting a link exists between JNK and $p27^{kip1}$ in migratory cells. Molecular mechanisms underlying the connections between JNK signaling, cytoskeletal modulators and other intrinsic features of interneuron migration remain to be determined.

In addition to intrinsic mechanisms, extrinsic influences on cortical interneuron migration may also be controlled by JNK. Indeed, we found greater disruptions to cortical interneuron migratory properties when *ex vivo* slices were treated with a JNK inhibitor than when interneurons were inhibited in the absence of all other cortical cells (compare Fig. 2M-P with 9H-K). This suggests that disruptions to JNK signaling may alter the environment that cortical interneurons travel through. Migrating cortical interneurons normally rely on cellular and molecular interactions with other cells to navigate into and within the cerebral cortex. For example, interneurons often reorient their mode of migration from tangential to radial after making contact with radial glia in the cortical wall (Yokota et al., 2007). Furthermore, disruptions to radial glia (Haubst et al., 2006; Talebian et al., 2017), cortical intermediate progenitors (Abe et al., 2015), cortical excitatory neurons (Hevner et al., 2004; Lodato et al., 2011; Pla et al., 2006), microglia (Squarzoni et al., 2014), blood vessels (Barber et al., 2018) and thalamocortical axons (Zechel et al., 2016) all have a non-autonomous effect on the migration of cortical interneurons. Therefore, if JNK activity is

Development (2020) 147, dev180646. doi:10.1242/dev.180646

required for the normal development of these cellular components of the cortical environment, as is the case for radially migrating cortical excitatory neurons (Westerlund et al., 2011; Zhang et al., 2016), JNK disruption may non-autonomously impact interneuron migration.

In pharmacologically treated and genetically manipulated *ex vivo* slices, interneurons adopted non-tangential trajectories and prematurely departed from migratory streams, indicating that both approaches used to eliminate JNK function yielded consistent results. However, we found that interneurons in JNK-inhibited slices displayed greater alterations in migratory properties, which led to faster and more complete disruption of migratory streams. This could be explained by inherent differences in acute pharmacological inhibition, where JNK signaling is abruptly abrogated, versus chronic genetic loss, where JNK removal may be compensated for over time. Alternatively, as all three Jnk proteins are globally inhibited after SP600125 treatment while *Jnk1* is retained in *Dlx5/6-CIE*-negative cells of *cTKO* cortices, Jnk1 function in non-interneuronal cells of the genetic model may lessen the severity of interneuron phenotypes. Thus, regardless of how differences between pharmacological and genetic manipulations originate, JNK function in other cell types should be carefully considered.

Finally, our data suggest that *Jnk2* and *Jnk3* are not crucial for the normal allocation of cortical interneurons at P0. However, we cannot exclude the possibility that the *Jnk2*- and *Jnk3*-deficient environment of *cTKO* brains does not further compromise the migration and allocation of JNK-depleted interneurons. Moreover, as JNK is conditionally deleted in ventral forebrain progenitors of the *cTKO* brain, we cannot exclude the possibility that aberrant subcortical migration or delayed entry into the cortical rudiment impacts subsequent allocation of interneurons in the cortical wall. More sophisticated *in utero* manipulation experiments designed to eliminate JNK activity from cortical interneurons only after they have entered the cortex are needed to address the autonomous and temporal requirements for JNK in interneuron migration and allocation.

Conclusions and future perspectives

We have found a novel requirement for JNK signaling in cortical interneuron stream maintenance, interneuron migratory behavior and morphology, and the laminar distribution of interneurons in the cortical wall. These findings are significant, as even minor disruptions to the migration of cortical interneurons have been implicated in the etiology of severe neurological and neuropsychiatric disorders (Dubos et al., 2018; Meechan et al., 2012; Volk et al., 2015). Therefore, elucidating upstream activators and downstream effectors of JNK signaling in cortical interneurons will be essential for determining extrinsic and intrinsic functions of JNK in cortical development, and could help to unravel complex neurodevelopmental disorders that impinge upon the formation and function of the cerebral cortex.

MATERIALS AND METHODS

Animals

Mice (*Mus musculus*) were housed and cared for by the Office of Laboratory Animal Resources at West Virginia University. Timed-pregnant dams [day of vaginal plug=embryonic (E) day 0.5] were euthanized by rapid cervical dislocation, and mouse embryos were immediately harvested for tissue culture or histological analyses. For *ex vivo* pharmacological slice culture experiments, CF-1 (Charles River) dams were crossed to hemizygous *Dlx5/6-Cre-IRES-EGFP* [*Dlx5/6-CIE*; (Stenman et al., 2003)] males maintained on a C57BL/6J (stock 000664, The Jackson Laboratory) background to achieve timed pregnancies at E14.5. For medial ganglionic eminence (MGE) explant assays, C57BL/6J dams were crossed to *Dlx5/6-CIE* males. For *in vivo* genetic knockout experiments, as well as *ex vivo* slice cultures using genetic knockout material, new mouse strains were established and maintained on a C57BL/6J background. Floxed *Mapk8*^{tm1Rjd} mice (*Jnk1*$^{fl/fl}$; Das et al., 2007; kindly provided by Dr Roger Davis, University of Massachusetts Medical School, MA, USA) were bred with *Mapk9*^{tm1Flv} (*Jnk2*$^{-/-}$; stock 004321, The Jackson Laboratory), *Mapk10*^{tm1Flv} (*Jnk3*$^{-/-}$; stock 004322, The Jackson Laboratory) and/or *Dlx5/6-CIE* mice to generate breeding stock for genetic experiments. *Jnk1*$^{fl/fl}$; *Jnk2*$^{-/-}$ dams were mated with *Dlx5/6-CIE; Jnk1*$^{fl/+}$; *Jnk2*$^{-/-}$ males to generate conditional heterozygote knockout mice (*cHKO*: *Dlx5/6-CIE; Jnk1*$^{fl/+}$; *Jnk2*$^{-/-}$) and conditional double knockout mice (*cDKO*: *Dlx5/6-CIE; Jnk1*$^{fl/fl}$; *Jnk2*$^{-/-}$). *Jnk1*$^{fl/fl}$; *Jnk2*$^{-/-}$; *Jnk3*$^{-/-}$ dams were mated with *Dlx5/6-CIE; Jnk1*$^{fl/+}$; *Jnk2*$^{-/-}$; *Jnk3*$^{+/-}$ males to generate conditional triple knockout mice (*cTKO*: *Dlx5/6-CIE; Jnk1*$^{fl/fl}$; *Jnk2*$^{-/-}$; *Jnk3*$^{-/-}$), as well as *Dlx5/6-CIE; Jnk1*$^{fl/+}$; *Jnk2*$^{-/-}$; *Jnk3*$^{-/-}$ mice. To generate *Dlx5/6-CIE; Jnk2*$^{-/-}$; *Jnk3*$^{-/-}$ animals, *Jnk2*$^{+/-}$; *Jnk3*$^{-/-}$ dams were mated with *Dlx5/6-CIE; Jnk2*$^{-/-}$; *Jnk3*$^{+/-}$ males. P0 *Dlx5/6-CIE* animals were generated by crossing C57BL/6J dams with a *Dlx5/6-CIE* male. All animal procedures were performed as approved by the Institutional Animal Care and Use Committee at West Virginia University.

Organotypic slice cultures

Dlx5/6-CIE-positive embryos were collected at E14.5 and dissected in ice-cold complete HBSS (cHBSS; Tucker et al., 2006). The embryonic brains were embedded in a solution of 3% low melting point agarose (Fisher Scientific BP165-25) in cHBSS, sectioned coronally into 300 µm slices on a Leica VT1000 S vibratome, and transferred to poly-L-lysine/laminin-coated transwell membrane inserts in six-well plates (BD Falcon; Polleux and Ghosh, 2002). Each well was filled with 1.8 ml of slice culture media (Tucker et al., 2006) containing either dimethyl sulfoxide (DMSO, Sigma D2438) as a vehicle control or the pan-JNK inhibitor SP600125 (Enzo Life Sciences BML-EI305-0010) at a final concentration of 20 µM or 40 µM, as previously described (Myers et al., 2014). Slices were grown for 12 h for the pharmacological dose experiment (Fig. 1). For the washout experiment (Fig. 3), slices were grown for 12 h, the media containing the vehicle or the inhibitor was replaced, and the slices were grown for an additional 12 h.

3D Matrigel assay

Dlx5/6-CIE-positive embryos were collected at E14.5. MGE tissue was micro-dissected in ice-cold cHBSS, cut into small explants and stored in cHBSS on ice. Matrigel (Corning #356237) was combined 1:1 with serum-free media (Polleux and Ghosh, 2002), and 150 µl of the Matrigel mixture was added to each well of an 8-well chamber coverslip slide (Thermo Fisher 155411) on ice. Two or three MGE explants were placed at the bottom of each well near the coverslip. The slide was then transferred to a tissue culture incubator at 37°C with 5% CO_2 for 30 min to solidify the Matrigel mixture with the embedded explants. Warm serum-free media was added to each well and the explants were cultured for 24 h. After 24 h, serum-free media containing either control (DMSO) or SP600125 at a final concentration of 20 µM was added to each well immediately before imaging.

Live imaging

Live vibratome slices of E14.5 brains (prepared as above) were transferred to Millicell inserts (Millipore PICM0RG50) in a FluoroDish (World Precision Instruments FD35-100) either filled with 1.6 ml slice culture media for genetic knockout experiments, or filled with 1.6 ml slice culture media containing either control (DMSO) or 20 µM SP600125 for pharmacological experiments. FluoroDish preparations or Matrigel slides (prepared as above) were transferred to a Zeiss 710 confocal microscope equipped with stable environmental controls maintained at 37°C with 5% humidified CO_2. Multi-position time-lapse *z*-series were acquired every 10 min for 12-24 h with a LD Plan-Neofluar 20×/0.4 Korr objective lens for slices, and with a 20× Plan-Apo lens for the Matrigel experiments. The field of view was centered on the mid-point of the cortical wall for slices, and at the leading edge of interneuron outgrowth for the Matrigel explants. Tissue samples were collected from embryos for retrospective genotype identification.

Development (2020) 147, dev180646. doi:10.1242/dev.180646

Live-imaging analyses

4D live-imaging movies were analyzed using Imaris (Version 9.3.1) software by Bitplane. In slice culture assays, interneurons were tracked from left, center and right portions of the SVZ stream from movies recorded at the mid-cortical position. For selection, interneurons had to originate in the SVZ stream, migrate for at least 2 h, and be clearly distinguishable from surrounding cells. For Matrigel assays, interneurons had to migrate for a minimum of 4 h. All cell tracks were stopped when interneurons were no longer visible/distinguishable from nearby cells, if they stopped moving for a period of 60 min while being tracked or when the movie ended. For the pharmacological experiments, 12 interneurons were tracked from each of the 12 movies per condition (n=12), for a total of 144 tracks per condition. Movies were generated from at least seven different embryos per condition over three experimental days. For the genetic experiments, 10 interneurons were tracked from each of the 10 movies per genotype (n=10), for a total of 100 tracks per genotype in each of the three 6 h segments (300 tracks/genotype). Movies were generated from five different brains per genotype, collected over four experimental days. For the Matrigel experiment, 10 interneurons were tracked from each of the eight movies per condition (n=8), for a total of 80 tracks per condition, collected from three experiments. All tracks from each movie were averaged together for dynamic analyses. Cortical interneurons were tracked using the Spots feature of Imaris to capture migratory speed, distance, displacement and track straightness data, which were analyzed by two-tailed Student's t-tests. Displacement was normalized to the minimum track length (2 h slice culture, 4 h Matrigel) to account for differences in the total times of tracked cells. In addition, in the slice culture experiments, the direction of the leading processes of tracked cells was recorded each frame as tangential, diagonal or radial orientation. Overall differences in orientation were determined by two-way ANOVA followed by Fisher's LSD post-hoc analyses.

Tissue processing, cryosectioning and immunohistochemistry

E13.5 or E15.5 brains were dissected in phosphate-buffered saline (PBS; 136.9 mmol NaCl, 2.683 mmol KCl, 4.290 mmol Na_2HP0_4 $7H_2O$, 1.470 mmol KH_2P0_4) and immersion fixed with 4% paraformaldehyde (PFA) in PBS overnight at 4°C. Postnatal (P) day 0 pups were anesthetized on ice and transcardially perfused with chilled PBS followed by 4% PFA, and brains were dissected in PBS and immersion fixed overnight at 4°C. Samples were rinsed with PBS and progressed through a sucrose series (10%, 20% and 30%) prior to embedding. For fixed analyses of *ex vivo* slice cultures, slices were rinsed in PBS, fixed overnight in 4% PFA at 4°C, passaged through sucrose and re-embedded in agar sucrose (3.5% agar+8% sucrose) prior to removal from the transwell membrane. Both brains and slices were embedded in Tissue Freezing Medium (VWR 15146-019), flash frozen in liquid nitrogen-cooled 2-methyl butane (Fisher Scientific 03551-4) and stored at −80°C. Frozen brains and slice cultures were sectioned coronally at 12 µm on a Leica cryostat (CM 3050S), collected in series onto Superfrost Plus slides (Fisher Scientific 12-550-15) and stored at −20°C prior to use. Slides were rehydrated with PBS for 20 min and blocked for 2 h in permeability solution (Myers et al., 2014) with 5% normal goat serum. Primary antibodies, including chicken anti-GFP (1:1500, Abcam, ab13970) and rabbit anti-calbindin (1:2000, Swant, CB38) were diluted in permeability solution, applied to the slices and incubated overnight at 4°C. Slices were thoroughly rinsed in PBS and incubated with secondary antibodies, including Alexa 488-conjugated goat anti-chicken (1:4000, Invitrogen, A-11039) and Alexa 546-conjugated goat anti-rabbit (1:2000, Invitrogen, A-11010) diluted in permeability solution at room temperature for 2 h. Hoechst (Thermo Scientific 62249, 1 µg/ml) was used as a nuclear counterstain. Slices were rinsed in PBS, mounted in an aqueous mounting medium containing an anti-fade reagent and stored at 4°C.

Imaging and quantification of cryosectioned slices

Imaging

Immunofluorescently labeled cryosections of embryonic brain slices were imaged on a Zeiss 710 confocal microscope with a 20× Plan-Apo objective lens. P0 sections were imaged using an Olympus VS120 Slide Scanner with a UPLSAPO 10× objective. Confocal and slide scanned images were uniformly adjusted for levels, brightness and contrast in Adobe Photoshop.

Interneuron distribution

For quantifying radial distribution of interneurons, cropped regions of the cortical wall were equidistantly segmented into 10 bins from pial to ventricular surfaces (as in Fig. S1C,D). For quantifying interneuron entry into the cortex, the E13.5 cortical rudiment was divided into five equidistant bins (lateral to medial, as in Fig. 4D). For all experiments, the numbers of cells present in each equidistant bin were counted and their percentile distributions across all bins were determined for each tissue section. Bin distributions were averaged across sections of the same treatment group or genotype, and statistical significances were determined using two-way ANOVA followed by Fisher's LSD post-hoc analyses (GraphPad Prism 8). For E13.5 and E15.5 *in vivo* analyses, cropped regions from two hemi-sections were quantified at four predefined rostrocaudal locations, for a total of eight sections per brain (n=5 brains/genotype). At P0, three hemi-sections were selected from slices containing the anterior commissure region (n=3 or n=5 brains/genotype). In pharmacological experiments, four sections were used from each treated slice (n=5 brains/condition).

Interneuron morphology and leading process orientation

Interneuron morphologies were quantified by measuring the circularity of cell bodies and the length of leading processes in Adobe Photoshop. Leading process length was measured from clearly distinguishable cells located between the SVZ and MZ streams as a vector from the end of the cell body to the furthest point of the longest process. Two-tailed Student's t-tests were used to evaluate the statistical significance of morphological measurements between cells analyzed in each genotype. For both measurements, cells were selected from two hemi-sections per brain, at the same defined rostrocaudal location (n=5 brains/genotype). Orientation of leading processes was determined by measuring the angle of displacement from the tangential direction, which was defined as 0°. All angle measurements (n=5 brains/condition) were grouped into 12 different bins of 30° each, and statistical significances were determined by χ^2 analysis followed by Fisher's LSD post-hoc analyses (GraphPad Prism 8).

Acknowledgements

We thank Katie Padgett and Kelly Stake for their assistance in sample processing and data analysis, as well as Amanda Ammer and Karen Martin for their excellent microscopy support. Imaging experiments were performed in the West Virginia University (WVU) Imaging Facilities, which have been supported by the WVU Cancer Institute, the WVU HSC Office of Research and Graduate Education, and NIH grants P20RR016440, P30GM103488, P20GM121322, U54GM104942, P20GM10343 and P30GM103503.

Competing interests

The authors declare no competing or financial interests.

Author contributions

Conceptualization: A.K.M., E.S.T.; Methodology: A.K.M., J.G.C., E.S.T.; Formal analysis: A.K.M., J.G.C., S.E.S., J.P.S.; Investigation: A.K.M., J.G.C., S.E.S., J.P.S., C.A.S.; Writing - original draft: A.K.M.; Writing - review & editing: A.K.M., J.G.C., S.E.S., E.S.T.; Visualization: A.K.M., J.G.C., S.E.S.; Supervision: E.S.T.; Funding acquisition: E.S.T.

Funding

This work was supported by the National Institutes of Health (R01NS082262 to E.S.T.). Deposited in PMC for release after 12 months.

Supplementary information

Supplementary information available online at
http://dev.biologists.org/lookup/doi/10.1242/dev.180646.supplemental

References

Abe, P., Mueller, W., Schütz, D., MacKay, F., Thelen, M., Zhang, P. and Stumm, R. (2014). CXCR7 prevents excessive CXCL12-mediated downregulation of CXCR4 in migrating cortical interneurons. *Development* **141**, 1857-1863. doi:10.1242/dev.104224

Abe, P., Molnar, Z., Tzeng, Y.-S., Lai, D. M., Arnold, S. J. and Stumm, R. (2015). Intermediate progenitors facilitate intracortical progression of thalamocortical axons and interneurons through CXCL12 chemokine signaling. *J. Neurosci.* **35**, 13053-13063. doi:10.1523/JNEUROSCI.1488-15.2015

Barber, M., Andrews, W. D., Memi, F., Gardener, P., Ciantar, D., Tata, M., Ruhrberg, C. and Parnavelas, J. G. (2018). Vascular-derived vegfa promotes cortical interneuron migration and proximity to the vasculature in the developing forebrain. *Cereb. Cortex* **28**, 2577-2593. doi:10.1093/cercor/bhy082

Bartolini, G., Sánchez-Alcañiz, J. A., Osório, C., Valiente, M., García-Frigola, C. and Marín, O. (2017). Neuregulin 3 mediates cortical plate invasion and laminar allocation of GABAergic interneurons. *Cell Rep.* **18**, 1157-1170. doi:10.1016/j.celrep.2016.12.089

Baudoin, J.-P., Alvarez, C., Gaspar, P. and Métin, C. (2008). Nocodazole-induced changes in microtubule dynamics impair the morphology and directionality of migrating medial ganglionic eminence cells. *Dev. Neurosci.* **30**, 132-143. doi:10.1159/000109858

Baudoin, J.-P., Viou, L., Launay, P.-S., Luccardini, C., Espeso Gil, S., Kiyasova, V., Irinopoulou, T., Alvarez, C., Rio, J.-P., Boudier, T. et al. (2012). Tangentially migrating neurons assemble a primary cilium that promotes their reorientation to the cortical plate. *Neuron* **76**, 1108-1122. doi:10.1016/j.neuron.2012.10.027

Bellion, A., Baudoin, J. P., Alvarez, C., Bornens, M. and Metin, C. (2005). Nucleokinesis in tangentially migrating neurons comprises two alternating phases: forward migration of the Golgi/centrosome associated with centrosome splitting and myosin contraction at the rear. *J. Neurosci.* **25**, 5691-5699. doi:10.1523/JNEUROSCI.1030-05.2005

Bennett, B. L., Sasaki, D. T., Murray, B. W., O'Leary, E. C., Sakata, S. T., Xu, W., Leisten, J. C., Motiwala, A., Pierce, S., Satoh, Y. et al. (2001). SP600125, an anthrapyrazolone inhibitor of Jun N-terminal kinase. *Proc. Natl. Acad. Sci. USA* **98**, 13681-13686. doi:10.1073/pnas.251194298

Coffey, E. T. (2014). Nuclear and cytosolic JNK signalling in neurons. *Nat. Rev. Neurosci.* **15**, 285-299. doi:10.1038/nrn3729

Das, M., Jiang, F., Sluss, H. K., Zhang, C., Shokat, K. M., Flavell, R. A. and Davis, R. J. (2007). Suppression of p53-dependent senescence by the JNK signal transduction pathway. *Proc. Natl. Acad. Sci. USA* **104**, 15759-15764. doi:10.1073/pnas.0707782104

Davis, R. J. (2000). Signal transduction by the JNK group of MAP kinases. *Cell* **103**, 239-252. doi:10.1016/S0092-8674(00)00116-1

Décaillot, F. M., Kazmi, M. A., Lin, Y., Ray-Saha, S., Sakmar, T. P. and Sachdev, P. (2011). CXCR7/CXCR4 heterodimer constitutively recruits beta-arrestin to enhance cell migration. *J. Biol. Chem.* **286**, 32188-32197. doi:10.1074/jbc.M111.277038

Di Cristo, G. (2007). Development of cortical GABAergic circuits and its implications for neurodevelopmental disorders. *Clin. Genet.* **72**, 1-8. doi:10.1111/j.1399-0004.2007.00822.x

Dubos, A., Meziane, H., Iacono, G., Curie, A., Riet, F., Martin, C., Loaëc, N., Birling, M.-C., Selloum, M., Normand, E. et al. (2018). A new mouse model of ARX dup24 recapitulates the patients' behavioral and fine motor alterations. *Hum. Mol. Genet.* **27**, 2138-2153. doi:10.1093/hmg/ddy122

Elias, L. A. B., Turmaine, M., Parnavelas, J. G. and Kriegstein, A. R. (2010). Connexin 43 mediates the tangential to radial migratory switch in ventrally derived cortical interneurons. *J. Neurosci.* **30**, 7072-7077. doi:10.1523/JNEUROSCI.5728-09.2010

Flames, N., Long, J. E., Garratt, A. N., Fischer, T. M., Gassmann, M., Birchmeier, C., Lai, C., Rubenstein, J. L. and Marín, O. (2004). Short- and long-range attraction of cortical GABAergic interneurons by neuregulin-1. *Neuron* **44**, 251-261. doi:10.1016/j.neuron.2004.09.028

Friocourt, G., Liu, J. S., Antypa, M., Rakic, S., Walsh, C. A. and Parnavelas, J. G. (2007). Both doublecortin and doublecortin-like kinase play a role in cortical interneuron migration. *J. Neurosci.* **27**, 3875-3883. doi:10.1523/JNEUROSCI.4530-06.2007

Gdalyahu, A., Ghosh, I., Levy, T., Sapir, T., Sapoznik, S., Fishler, Y., Azoulai, D. and Reiner, O. (2004). DCX, a new mediator of the JNK pathway. *EMBO J.* **23**, 823-832. doi:10.1038/sj.emboj.7600079

Godin, J. D., Thomas, N., Laguesse, S., Malinouskaya, L., Close, P., Malaise, O., Purnelle, A., Raineteau, O., Campbell, K., Fero, M. et al. (2012). p27(Kip1) is a microtubule-associated protein that promotes microtubule polymerization during neuron migration. *Dev. Cell* **23**, 729-744. doi:10.1016/j.devcel.2012.08.006

Haubst, N., Georges-Labouesse, E., De Arcangelis, A., Mayer, U. and Gotz, M. (2006). Basement membrane attachment is dispensable for radial glial cell fate and for proliferation, but affects positioning of neuronal subtypes. *Development* **133**, 3245-3254. doi:10.1242/dev.02486

Hevner, R. F., Daza, R. A. M., Englund, C., Kohtz, J. and Fink, A. (2004). Postnatal shifts of interneuron position in the neocortex of normal and reeler mice: evidence for inward radial migration. *Neuroscience* **124**, 605-618. doi:10.1016/j.neuroscience.2003.11.033

Jin, J., Suzuki, H., Hirai, S., Mikoshiba, K. and Ohshima, T. (2010). JNK phosphorylates Ser332 of doublecortin and regulates its function in neurite extension and neuronal migration. *Dev. Neurobiol.* **70**, 929-942. doi:10.1002/dneu.20833

Kappeler, C., Saillour, Y., Baudoin, J.-P., Tuy, F. P. D., Alvarez, C., Houbron, C., Gaspar, P., Hamard, G., Chelly, J., Métin, C. et al. (2006). Branching and nucleokinesis defects in migrating interneurons derived from doublecortin knockout mice. *Hum. Mol. Genet.* **15**, 1387-1400. doi:10.1093/hmg/ddl062

Kato, M. and Dobyns, W. B. (2005). X-linked lissencephaly with abnormal genitalia as a tangential migration disorder causing intractable epilepsy: proposal for a new term, "interneuronopathy". *J. Child Neurol.* **20**, 392-397. doi:10.1177/08830738050200042001

Kim, H., Jung, O., Kang, M., Lee, M.-S., Jeong, D., Ryu, J., Ko, Y., Choi, Y.-J. and Lee, J. W. (2012). JNK signaling activity regulates cell-cell adhesions via TM4SF5-mediated p27(Kip1) phosphorylation. *Cancer Lett.* **314**, 198-205. doi:10.1016/j.canlet.2011.09.030

Kuan, C.-Y., Yang, D. D., Roy, D. R. S., Davis, R. J., Rakic, P. and Flavell, R. A. (1999). The Jnk1 and Jnk2 protein kinases are required for regional specific apoptosis during early brain development. *Neuron* **22**, 667-676. doi:10.1016/S0896-6273(00)80727-8

Li, G., Adesnik, H., Li, J., Long, J., Nicoll, R. A., Rubenstein, J. L. and Pleasure, S. J. (2008). Regional distribution of cortical interneurons and development of inhibitory tone are regulated by Cxcl12/Cxcr4 signaling. *J. Neurosci.* **28**, 1085-1098. doi:10.1523/JNEUROSCI.4602-07.2008

Liao, Y. X., Fu, Z. Z., Zhou, C. H., Shan, L. C., Wang, Z. Y., Yin, F., Zheng, L. P., Hua, Y. Q. and Cai, Z. D. (2015). AMD3100 reduces CXCR4-mediated survival and metastasis of osteosarcoma by inhibiting JNK and Akt, but not p38 or Erk1/2, pathways in in vitro and mouse experiments. *Oncol. Rep.* **34**, 33-42. doi:10.3892/or.2015.3992

Lodato, S., Rouaux, C., Quast, K. B., Jantrachotechatchawan, C., Studer, M., Hensch, T. K. and Arlotta, P. (2011). Excitatory projection neuron subtypes control the distribution of local inhibitory interneurons in the cerebral cortex. *Neuron* **69**, 763-779. doi:10.1016/j.neuron.2011.01.015

Lopez-Bendito, G., Sánchez-Alcaniz, J. A., Pla, R., Borrell, V., Pico, E., Valdeolmillos, M. and Marín, O. (2008). Chemokine signaling controls intracortical migration and final distribution of GABAergic interneurons. *J. Neurosci.* **28**, 1613-1624. doi:10.1523/JNEUROSCI.4651-07.2008

Lysko, D. E., Putt, M. and Golden, J. A. (2011). SDF1 regulates leading process branching and speed of migrating interneurons. *J. Neurosci.* **31**, 1739-1745. doi:10.1523/JNEUROSCI.3118-10.2011

Lysko, D. E., Putt, M. and Golden, J. A. (2014). SDF1 reduces interneuron leading process branching through dual regulation of actin and microtubules. *J. Neurosci.* **34**, 4941-4962. doi:10.1523/JNEUROSCI.4351-12.2014

Marín, O. (2012). Interneuron dysfunction in psychiatric disorders. *Nat. Rev. Neurosci.* **13**, 107-120. doi:10.1038/nrn3155

Martini, F. J. and Valdeolmillos, M. (2010). Actomyosin contraction at the cell rear drives nuclear translocation in migrating cortical interneurons. *J. Neurosci.* **30**, 8660-8670. doi:10.1523/JNEUROSCI.1962-10.2010

Meechan, D. W., Tucker, E. S., Maynard, T. M. and LaMantia, A.-S. (2012). Cxcr4 regulation of interneuron migration is disrupted in 22q11.2 deletion syndrome. *Proc. Natl. Acad. Sci. USA* **109**, 18601-18606. doi:10.1073/pnas.1211507109

Miyoshi, G. and Fishell, G. (2011). GABAergic interneuron lineages selectively sort into specific cortical layers during early postnatal development. *Cereb. Cortex* **21**, 845-852. doi:10.1093/cercor/bhq155

Miyoshi, G., Hjerling-Leffler, J., Karayannis, T., Sousa, V. H., Butt, S. J. B., Battiste, J., Johnson, J. E., Machold, R. P. and Fishell, G. (2010). Genetic fate mapping reveals that the caudal ganglionic eminence produces a large and diverse population of superficial cortical interneurons. *J. Neurosci.* **30**, 1582-1594. doi:10.1523/JNEUROSCI.4515-09.2010

Myers, A. K., Meechan, D. W., Adney, D. R. and Tucker, E. S. (2014). Cortical interneurons require Jnk1 to enter and navigate the developing cerebral cortex. *J. Neurosci.* **34**, 7787-7801. doi:10.1523/JNEUROSCI.4695-13.2014

Nery, S., Fishell, G. and Corbin, J. G. (2002). The caudal ganglionic eminence is a source of distinct cortical and subcortical cell populations. *Nat. Neurosci.* **5**, 1279-1287. doi:10.1038/nn971

Petrich, B. G., Gong, X., Lerner, D. L., Wang, X., Brown, J. H., Saffitz, J. E. and Wang, Y. (2002). c-Jun N-terminal kinase activation mediates downregulation of connexin43 in cardiomyocytes. *Circ. Res.* **91**, 640-647. doi:10.1161/01.RES.0000035854.11082.01

Pla, R., Borrell, V., Flames, N. and Marin, O. (2006). Layer acquisition by cortical GABAergic interneurons is independent of Reelin signaling. *J. Neurosci.* **26**, 6924-6934. doi:10.1523/JNEUROSCI.0245-06.2006

Polleux, F. and Ghosh, A. (2002). The slice overlay assay: a versatile tool to study the influence of extracellular signals on neuronal development. *Sci. STKE* **2002**, pl9. doi:10.1126/stke.2002.136.pl9

Sánchez-Alcaniz, J. A., Haege, S., Mueller, W., Pla, R., Mackay, F., Schulz, S., López-Bendito, G., Stumm, R. and Marin, O. (2011). Cxcr7 controls neuronal migration by regulating chemokine responsiveness. *Neuron* **69**, 77-90. doi:10.1016/j.neuron.2010.12.006

Squarzoni, P., Oller, G., Hoeffel, G., Pont-Lezica, L., Rostaing, P., Low, D., Bessis, A., Ginhoux, F. and Garel, S. (2014). Microglia modulate wiring of the embryonic forebrain. *Cell Rep* **8**, 1271-1279. doi:10.1016/j.celrep.2014.07.042

Stenman, J., Toresson, H. and Campbell, K. (2003). Identification of two distinct progenitor populations in the lateral ganglionic eminence: implications for striatal and olfactory bulb neurogenesis. *J. Neurosci.* **23**, 167-174. doi:10.1523/JNEUROSCI.23-01-00167.2003

Stumm, R. K., Zhou, C., Ara, T., Lazarini, F., Dubois-Dalcq, M., Nagasawa, T., Höllt, V. and Schulz, S. (2003). CXCR4 regulates interneuron migration in the

developing neocortex. *J. Neurosci.* **23**, 5123-5130. doi:10.1523/JNEUROSCI.23-12-05123.2003

Talebian, A., Britton, R., Ammanuel, S., Bepari, A., Sprouse, F., Birnbaum, S. G., Szabó, G., Tamamaki, N., Gibson, J. and Henkemeyer, M. (2017). Autonomous and non-autonomous roles for ephrin-B in interneuron migration. *Dev. Biol.* **431**, 179-193. doi:10.1016/j.ydbio.2017.09.024

Tham, T. N., Lazarini, F., Franceschini, I. A., Lachapelle, F., Amara, A. and Dubois-Dalcq, M. (2001). Developmental pattern of expression of the alpha chemokine stromal cell-derived factor 1 in the rat central nervous system. *Eur. J. Neurosci.* **13**, 845-856. doi:10.1046/j.0953-816x.2000.01451.x

Tiveron, M.-C., Rossel, M., Moepps, B., Zhang, Y. L., Seidenfaden, R., Favor, J., Konig, N. and Cremer, H. (2006). Molecular interaction between projection neuron precursors and invading interneurons via stromal-derived factor 1 (CXCL12)/CXCR4 signaling in the cortical subventricular zone/intermediate zone. *J. Neurosci.* **26**, 13273-13278. doi:10.1523/JNEUROSCI.4162-06.2006

Tucker, E. S., Polleux, F. and LaMantia, A.-S. (2006). Position and time specify the migration of a pioneering population of olfactory bulb interneurons. *Dev. Biol.* **297**, 387-401. doi:10.1016/j.ydbio.2006.05.009

Volk, D. W., Chitrapu, A., Edelson, J. R. and Lewis, D. A. (2015). Chemokine receptors and cortical interneuron dysfunction in schizophrenia. *Schizophr. Res.* **167**, 12-17. doi:10.1016/j.schres.2014.10.031

Wang, Y., Li, G., Stanco, A., Long, J. E., Crawford, D., Potter, G. B., Pleasure, S. J., Behrens, T. and Rubenstein, J. L. R. (2011). CXCR4 and CXCR7 have distinct functions in regulating interneuron migration. *Neuron* **69**, 61-76. doi:10.1016/j.neuron.2010.12.005

Westerlund, N., Zdrojewska, J., Padzik, A., Komulainen, E., Björkblom, B., Rannikko, E., Tararuk, T., Garcia-Frigola, C., Sandholm, J., Nguyen, L. et al. (2011). Phosphorylation of SCG10/stathmin-2 determines multipolar stage exit and neuronal migration rate. *Nat. Neurosci.* **14**, 305-313. doi:10.1038/nn.2755

Xu, Q., Cobos, I., De La Cruz, E., Rubenstein, J. L. and Anderson, S. A. (2004). Origins of cortical interneuron subtypes. *J. Neurosci.* **24**, 2612-2622. doi:10.1523/JNEUROSCI.5667-03.2004

Yau, H.-J., Wang, H. F., Lai, C. and Liu, F. C. (2003). Neural development of the neuregulin receptor ErbB4 in the cerebral cortex and the hippocampus: preferential expression by interneurons tangentially migrating from the ganglionic eminences. *Cereb. Cortex* **13**, 252-264. doi:10.1093/cercor/13.3.252

Yokota, Y., Gashghaei, H. T., Han, C., Watson, H., Campbell, K. J. and Anton, E. S. (2007). Radial glial dependent and independent dynamics of interneuronal migration in the developing cerebral cortex. *PLoS ONE* **2**, e794. doi:10.1371/journal.pone.0000794

Zechel, S., Nakagawa, Y. and Ibanez, C. F. (2016). Thalamo-cortical axons regulate the radial dispersion of neocortical GABAergic interneurons. *Elife* **5**, e20770. doi:10.7554/eLife.20770.025

Zhang, F., Yu, J., Yang, T., Xu, D., Chi, Z., Xia, Y. and Xu, Z. (2016). A novel c-Jun N-terminal Kinase (JNK) signaling complex involved in neuronal migration during brain development. *J. Biol. Chem.* **291**, 11466-11475. doi:10.1074/jbc.M116.716811